

# The molecular nature of superfluidity: Viscosity of helium from quantum stochastic molecular dynamics simulations over real trajectories

Phil Attard

phil.attard1@gmail.com July, October, 2024

Using quantum equations of motion for interacting bosons, stochastic molecular dynamics simulations with quantized momenta are performed for Lennard-Jones helium-4. The viscosity of the quantum liquid is significantly less than that of the classical liquid, being almost 5 times smaller at the lowest temperature studied. The classical and quantum liquids are identical except for Bose-Einstein condensation, which pinpoints the molecular mechanism for superfluidity. The results rely on the existence of stochastic but real particle trajectories, which has implications for the interpretation of quantum mechanics.

## I. INTRODUCTION

Shut up and calculate (1.1)

is an aphorism apparently due to Mermin, although some say Feynman (Mermin 1989, 2004). The sentiment, which is widespread and likely predates the specific phrase, suggests that it is a waste of time to speculate about the interpretation of quantum mechanics since everyone agrees upon the fundamental equations. It acknowledges the spookiness of quantum non-locality and the jittery state of Schrödinger's cat, but it insists that the physical meaning of these has no bearing on the application of the quantum laws and equations, which themselves are unambiguous.

It is certainly true that any theory or calculation is bound by the mathematical rules. Nevertheless I think that it goes too far to say that the physical interpretation of those rules is irrelevant or that the discussion of fundamental quantum concepts is mere sophistry. Once one goes beyond the highly idealized undergraduate textbook examples to work on real world problems, it is necessary to introduce approximations into the fundamental quantum equations. Such approximations may involve neglecting particular classes of terms while resumming others, defining parameters and taking small or large asymptotic limits, choosing specific functions for expansion series, imposing particular boundary conditions, etc. The approach chosen depends not just upon the physical characteristics of the problem at hand but also upon the interpretation of quantum mechanics that leads to an understanding of what is important and what is negligible, what is doable and what is forbidden. It is often the case that the real world application is so far removed from the fundamental quantum equations that the results of an early decision for the research direction cannot be fully anticipated or easily undone. Different interpretations can lead to widely divergent theories due to the sensitivity to the initial beliefs, if you will.

Let me give a concrete example that is directly relevant to the present paper on computing the viscosity of

helium in the superfluid regime. The Copenhagen interpretation of quantum mechanics holds that the world is not objectively real and that it only comes into existence when it is measured or observed. More specifically, particles only possess position or momentum at the time of measurement, and that only one of these can be measured at a time. Therefore, it is said, a particle does not possess simultaneously position and momentum. The corollary of this is that particles cannot follow a path from one position-momentum point to another, which is to say that particle trajectories do not exist.

Obviously any scientist who wishes to understand superfluidity at the molecular level and who believes in the Copenhagen interpretation of quantum mechanics would never consider developing a theory or approximation that is based upon real particles with actual positions and momenta following actual trajectories in time. This example illustrates how a particular interpretation of quantum mechanics can proscribe from the start the theories or approximations that are even considered, let alone explored.

The results in this paper are based on real particles with simultaneously specified positions and momenta, and on real molecular trajectories in time. These obviously contradict the Copenhagen interpretation of quantum mechanics. But do they contradict the equations of quantum mechanics? Obviously I argue not, as I now briefly explain.

It is certainly true that the position and momentum operators do not commute and that Heisenberg's uncertainty principle bounds the product of the variance of the expectation values of the position and momentum operators. These are indisputable mathematical facts. Anything beyond these is a matter of interpretation, and highly questionable interpretation at that. For example, the assertion that an expectation value is a measurement is dubious; there are entire journals devoted to the quantum theory of measurement and the only thing that the various authors agree upon is that a measurement is not simply an expectation value. Further, it is not at all clear that the lack of commutativity of the position and momentum operators implies the Copenhagen interpre-

tation that a particle cannot possess simultaneously a position and a momentum. For a counter-example, see the de Broglie-Bohm pilot wave theory, which reproduces all of the known results of quantum mechanics (Bohm 1952, de Broglie 1928, Goldstein 2024).

The approach used here is predicated on the interpretation that it is the momentum eigenvalue that gives the momentum of a particle, and that a momentum eigenfunction at a particular position should be interpreted as a complex number that is associated with the simultaneous specification of the position and momentum of the particle. In a way that will be made clear, the state of the system is the product of single-particle momentum eigenfunctions of the subsystem, and the subsystem evolves in time by following a trajectory through classical phase space as given by the Schrödinger equation applied to the momentum eigenfunctions and taking into account the interactions with the environment. It is essential to this approach that the subsystem of interest be open and that it can exchange energy and momentum with its environment. (The total system consists of the subsystem and the reservoir or environment.) It is also essential that the symmetrization of the wave function be explicitly accounted for.

At the end of the day, the present interpretation and the consequent approximations that are made should be judged by their physical plausibility and by the results that they produce. One cannot really maintain that the interpretation of quantum mechanics is irrelevant to the real world if the same starting equations combined with different interpretations lead to different quantitative descriptions of that world. The present approach gives a quantitative estimate of the shear viscosity of superfluid helium that includes molecular interactions. Apart from related work by the present author (Attard 2023b, 2025), these are the first such molecular-level results for the superfluid viscosity. It is therefore reasonable to conclude that the proximal impediment to the molecular understanding and quantitative description of superfluidity has been the Copenhagen interpretation of quantum mechanics.

## II. ANALYSIS

### A. Non-local Dynamics

I have previously given a formally exact formulation of quantum statistical mechanics in classical phase space (Attard 2018, 2021, 2023a). Decoherence due to entanglement with the reservoir or environment is essential to the formulation. In this the configuration picture I rely upon the momentum eigenfunction  $\phi_{\mathbf{p}}(\mathbf{q}) = V^{-N/2} e^{-\mathbf{p} \cdot \mathbf{q} / i\hbar}$  (Merzbacher 1970, Messiah 1961). Here for  $N$  particles the momentum configuration is  $\mathbf{p} = \{\mathbf{p}_1, \mathbf{p}_2, \dots, \mathbf{p}_N\}$ , and the position configuration is  $\mathbf{q} = \{\mathbf{q}_1, \mathbf{q}_2, \dots, \mathbf{q}_N\}$ . The momenta are quantized, with momentum state spacing  $\Delta_p = 2\pi\hbar/L$ , with  $V = L^3$  being

the volume of the cubic subsystem, and  $\hbar = 1.05 \times 10^{-34}$  being Planck's constant divided by  $2\pi$ . The spacing between momentum states goes to zero in the thermodynamic limit. Note that a point in classical phase space,  $\mathbf{\Gamma} \equiv \{\mathbf{q}, \mathbf{p}\}$ , has the interpretation of a specific configuration of bosons at these positions with these (quantized) momenta, and it has associated with it the complex number  $\phi_{\mathbf{p}}(\mathbf{q})$ .

For bosons the normalized symmetrized momentum eigenfunction is

$$\phi_{\mathbf{p}}^+(\mathbf{q}) = \frac{1}{\sqrt{N! \chi_{\mathbf{p}}^+}} \sum_{\hat{\mathbf{p}}} \phi_{\hat{\mathbf{p}}\mathbf{p}}(\mathbf{q}), \quad (2.1)$$

$\hat{\mathbf{p}}$  being the permutation operator. The symmetrization factor is

$$\begin{aligned} \chi_{\mathbf{p}}^+ &= \sum_{\hat{\mathbf{p}}} \langle \phi_{\mathbf{p}} | \phi_{\hat{\mathbf{p}}\mathbf{p}} \rangle \\ &= \sum_{\hat{\mathbf{p}}} \delta_{\mathbf{p}, \hat{\mathbf{p}}\mathbf{p}} \\ &= \prod_{\mathbf{a}} N_{\mathbf{a}}(\mathbf{p})!. \end{aligned} \quad (2.2)$$

Here and throughout the occupancy of the single particle momentum state  $\mathbf{a}$  is  $N_{\mathbf{a}} = \sum_{j=1}^N \delta_{\mathbf{p}_j, \mathbf{a}}$ . This is what ultimately drives Bose-Einstein condensation (Attard 2025). The formulation of quantum statistical mechanics relies upon the fact that the subsystem is decoherent due to entanglement with the reservoir or environment.

The Born probability associated with a point in classical phase space for the subsystem in a symmetrized decoherent momentum state is (Attard 2025 Eq. (5.67))

$$\begin{aligned} &\phi_{\mathbf{p}}^+(\mathbf{q})^* \phi_{\mathbf{p}}^+(\mathbf{q}) \\ &= \frac{1}{V^N N! \chi_{\mathbf{p}}^+} \sum_{\hat{\mathbf{p}}', \hat{\mathbf{p}}''} e^{-(\hat{\mathbf{p}}'\mathbf{p} - \hat{\mathbf{p}}''\mathbf{p}) \cdot \mathbf{q} / i\hbar} \\ &\approx \frac{1}{V^N N! \chi_{\mathbf{p}}^+} \sum_{\hat{\mathbf{p}}', \hat{\mathbf{p}}''}^{(\hat{\mathbf{p}}'\mathbf{p} \approx \hat{\mathbf{p}}''\mathbf{p})} e^{-(\hat{\mathbf{p}}'\mathbf{p} - \hat{\mathbf{p}}''\mathbf{p}) \cdot \mathbf{q} / i\hbar}. \end{aligned} \quad (2.3)$$

The reason for neglecting the terms involving permutations of bosons with dissimilar momenta is that these are more or less randomly and uniformly distributed on the unit circle in the complex plane, and so they add up to zero. This is particularly the case when one considers that small changes in the positions may lead to wildly different exponents for any such permutations. The sum that is retained involves only permutations between bosons in the same, or nearly the same, momentum state, in which case the exponent is zero, or close to zero, even for small changes in positions. The number of permutations between bosons in exactly the same momentum states in the double sum is  $\sum_{\hat{\mathbf{p}}', \hat{\mathbf{p}}''}^{(\hat{\mathbf{p}}'\mathbf{p} = \hat{\mathbf{p}}''\mathbf{p})} = N! \prod_{\mathbf{a}} N_{\mathbf{a}}(\mathbf{p})! = N! \chi_{\mathbf{p}}^+$ . Arguably these are the ones that dominate, with the permutations

between bosons in neighboring momentum states providing a correction.

An open system is decoherent (Attard 2018, 2021, Joos and Zeh 1985, Schlosshauer 2005, Zurek 1991). Decoherence means that the only allowed permutations must satisfy  $\hat{P}\mathbf{p} = \mathbf{p}$ . Otherwise the symmetrized momentum eigenfunction,  $\phi_{\mathbf{p}}^+(\mathbf{q})$ , would be a superposition of states.

There is a decoherence time  $\tau_{\text{mix}}$  (Caldeira and Leggett 1983, Schlosshauer 2005, Zurek *et al.* 2003). This likely decreases with increasing distance between permuted momentum states.

Schrödinger's equation for the time evolution of the momentum eigenfunction in a decoherent system for a small time step gives (Attard 2023d, 2025),

$$[\hat{I} + (\tau/i\hbar)\hat{\mathcal{H}}(\mathbf{q})]\phi_{\mathbf{p}}(\mathbf{q}) = \phi_{\bar{\mathbf{p}}}(\bar{\mathbf{q}}). \quad (2.4)$$

Time reversibility and continuity imply that

$$\begin{aligned} \bar{\mathbf{q}}' &= \mathbf{q} + \tau\nabla_{\mathbf{p}}\mathcal{H}(\mathbf{q}, \mathbf{p}), \\ \text{and } \bar{\mathbf{p}}' &= \mathbf{p} - \tau\nabla_{\mathbf{q}}\mathcal{H}(\mathbf{q}, \mathbf{p}). \end{aligned} \quad (2.5)$$

These are Hamilton's classical equations of motion. The second says that a boson's momentum evolves according to the classical force acting on it.

Focussing on the occupied momentum state  $\mathbf{a}$ , consecutive permutations of the  $N_{\mathbf{a}}$  bosons initially in it has over a time  $\tau \gtrsim \tau_{\text{mix}}$  the effect of sharing equally the classical forces acting on them. On average they therefore evolve classically together, each under the influence of identical non-local forces. The dynamics of a momentum state are those of a rigid body, except that the bosons respond to the equally shared non-local forces on an individual stochastic basis (see the next section).

In detail, for short time intervals,  $\tau < \tau_{\text{mix}}$ , the subsystem can exist in a superposition of permutations of nearby momentum states as each evolves according to local forces. Eventually, however, for  $\tau > \tau_{\text{mix}}$  this has to be winnowed down to a small window about a single pure state. This state must satisfy  $\hat{P}\bar{\mathbf{p}}'(\tau|\mathbf{q}, \mathbf{p}) = \bar{\mathbf{p}}'(\tau|\mathbf{q}, \mathbf{p})$ , for any permutation  $\hat{P}$  such that  $\hat{P}\mathbf{p} = \mathbf{p}$ . This is the state predicted by the non-local force per boson in the initial momentum state. In the random phase analysis of the Born probability above, amongst all the superposed states, the one with the bosons all in the same new momentum state is the one with the greatest weight.

To put it another way, the original momentum configuration with  $N_{\mathbf{a}}$  bosons in the momentum state  $\mathbf{a}$  evolves along initially  $N_{\mathbf{a}}!$  trajectories according to the classical local forces. These trajectories, or the configurations on them, are superposed. Each configuration in the superposition then bifurcates into  $N_{\mathbf{a}}!$  further trajectories. Thus the number of superposed trajectories grows exponentially. These trajectories diverge from each other in momentum space, and the most divergent are most quickly culled by the mechanism of decoherence. The trajectories that come to dominate are those that are closest together, which eventually means the one with all the  $N_{\mathbf{a}}$  bosons in the same momentum state (cf. Fig. 1). This

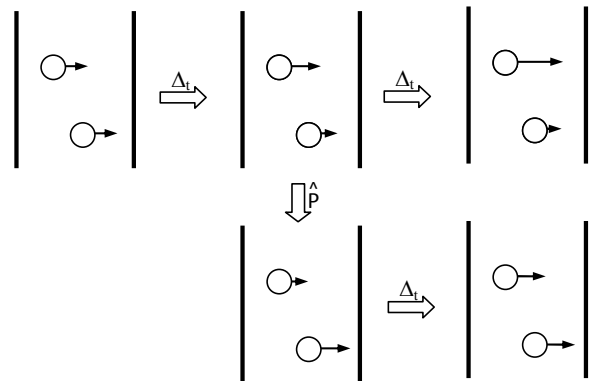


FIG. 1: Two bosons moving near repulsive walls. The bosons are initially in the same momentum state (left). After an intermediate transposition (middle), the final configuration with equal momenta (lower right) has double weight due to its identical transpose. The final configuration with different momenta (upper right) partly cancels with its transpose.

is the trajectory that results from all the bosons sharing equally over the time interval the local forces acting on each of them individually.

Of course from the classical perspective, in the thermodynamic limit the spacing between momentum states becomes infinitesimal, and there is no measurable distinction between the subsystem being in a momentum configuration and being in a superposition of neighboring momentum configurations.

The shared non-local force per boson in momentum state  $\mathbf{a}$  is (Attard 2025)

$$\mathbf{F}_{\mathbf{a}} = \frac{1}{N_{\mathbf{a}}} \sum_{j \in \mathbf{a}} \mathbf{f}_j. \quad (2.6)$$

Here the local classical force on boson  $j$  is  $\mathbf{f}_j = -\nabla_{\mathbf{q},j}U(\mathbf{q})$ , where  $U(\mathbf{q})$  is the potential energy. The permutation of the momenta of the bosons in a momentum state effectively averages the local forces and applies it non-locally across the momentum state.

The occupation entropy,  $S^{\text{occ}}(\mathbf{p}) = k_{\text{B}} \ln \chi_{\mathbf{p}}^+$ , acts like an additional force that seeks to keep bosons together in the same momentum state. The shared non-local force preserves the occupation entropy on average.

It should be emphasized that there are two sources of decoherence: there is the internal decoherence that was discussed above on the basis of the Born probability, and there is the eternal decoherence due to the entanglement of the open subsystem with the environment or reservoir. Both mechanisms dictate that the subsystem must be in a pure state where each boson has a position and a momentum. Allowed permutations are between bosons in the same momentum state, and, for limited time periods, also between bosons in neighboring momentum states. Permutations between bosons in different momentum states, which would correspond to the superposition of different momentum configurations, are suppressed, with the sup-

pression increasing with increasing distance between the permuted states.

### B. Adiabatic Transition

The change in position of the bosons over a time step  $\tau$  is deterministic,

$$\mathbf{q}(t + \tau) = \mathbf{q}(t) + \frac{\tau}{m} \mathbf{p}(t). \quad (2.7)$$

The momenta are quantized, with  $\mathbf{p}$  being a  $3N$ -dimensional vector integer multiple of  $\Delta_p$ .

Consider the transition of a single boson in the momentum state  $\mathbf{a}$ , which has  $N_{\mathbf{a}}$  bosons, to a neighboring momentum state  $\mathbf{a}'$ , which has  $N_{\mathbf{a}'}$  bosons,  $\{N_{\mathbf{a}}, N_{\mathbf{a}'}\} \xrightarrow{\tau} \{N_{\mathbf{a}} - 1, N_{\mathbf{a}'} + 1\}$ . The conditional transition probability for the time step gives the transition rate. Bayes theorem for the conditional transition probability with microscopic reversibility is (Attard 2012a)

$$\begin{aligned} & \varphi(N_{\mathbf{a}} - 1, N_{\mathbf{a}'} + 1; t + \tau | N_{\mathbf{a}}, N_{\mathbf{a}'}; t) \varphi(N_{\mathbf{a}}, N_{\mathbf{a}'}; t) \\ &= \varphi(N_{-\mathbf{a}}, N_{-\mathbf{a}'}; t | N_{-\mathbf{a}} - 1, N_{-\mathbf{a}'} + 1; t - \tau) \\ & \quad \times \varphi(N_{-\mathbf{a}} - 1, N_{-\mathbf{a}'} + 1; t - \tau), \end{aligned} \quad (2.8)$$

or

$$\begin{aligned} & \frac{\varphi(N_{-\mathbf{a}} - 1, N_{-\mathbf{a}'} + 1; t - \tau)}{\varphi(N_{\mathbf{a}}, N_{\mathbf{a}'}; t)} \\ &= \frac{\varphi(N_{\mathbf{a}} - 1, N_{\mathbf{a}'} + 1; t | N_{\mathbf{a}}, N_{\mathbf{a}'}; t - \tau)}{\varphi(N_{-\mathbf{a}}, N_{-\mathbf{a}'}; t + \tau | N_{-\mathbf{a}} - 1, N_{-\mathbf{a}'} + 1; t)}. \end{aligned} \quad (2.9)$$

If all of the momenta are reversed,  $\mathbf{p} \Rightarrow -\mathbf{p}$ , then  $N_{-\mathbf{a}} = N_{\mathbf{a}}$  and  $N_{-\mathbf{a}'} = N_{\mathbf{a}'}$ .

The change in potential energy due to the motion of the single boson under consideration during the time step is

$$\begin{aligned} & U(\mathbf{q}(-\mathbf{a}', t - \tau)) - U(\mathbf{q}) \\ &= U(\mathbf{q} + \tau \mathbf{a}'/m) - U(\mathbf{q}) \\ &= \frac{-\tau}{m} \mathbf{F}_{\mathbf{a}} \cdot \mathbf{a}' \\ &= \frac{-\tau}{m} \mathbf{F}_{\mathbf{a}} \cdot \mathbf{a} + \mathcal{O}(\tau \tilde{\Delta}_p). \end{aligned} \quad (2.10)$$

Notice that this takes boson  $j \in \mathbf{a}$  to experience the shared non-local force per boson,  $\mathbf{F}_{\mathbf{a}} = N_{\mathbf{a}}^{-1} \sum_{k \in \mathbf{a}} \mathbf{f}_k(\mathbf{q})$ , rather than  $\mathbf{f}_j$ , the local classical force. The total change in potential energy due to bosons in the momentum state  $\mathbf{a}$  obtained with the shared non-local force is the same as would have been obtained summing over the change due to the individual local classical forces.

With this, in the occupancy picture (Attard 2021, 2023a, 2025, Pathria 1972), the left hand side of Bayes'

theorem is

$$\begin{aligned} & \frac{\varphi(N_{-\mathbf{a}} - 1, N_{-\mathbf{a}'} + 1; t - \tau)}{\varphi(N_{\mathbf{a}}, N_{\mathbf{a}'}; t)} \\ &= \frac{\varphi(N_{\mathbf{a}} - 1, N_{\mathbf{a}'} + 1; t - \tau)}{\varphi(N_{\mathbf{a}}, N_{\mathbf{a}'}; t)} \\ &= e^{-\beta[a'^2 - a^2]/2m} e^{\beta \tau \mathbf{F}_{\mathbf{a}} \cdot \mathbf{a}/m} \\ &\approx 1 - \frac{\beta}{m} [\mathbf{a}' - \mathbf{a}] \cdot \mathbf{a} + \frac{\beta \tau}{m} \mathbf{F}_{\mathbf{a}} \cdot \mathbf{a} \\ & \quad + \mathcal{O}(\tilde{\Delta}_p^2) + \mathcal{O}(\tau^2) + \mathcal{O}(\tilde{\Delta}_p \tau). \end{aligned} \quad (2.11)$$

This is the occupancy picture and there is no occupation entropy. Most commonly the transition is to the nearest neighbor state,  $\tilde{\Delta}_p = \Delta_p$ . But as discussed below there may be occasions when it is necessary to jump further afield, in which case  $\tilde{\Delta}_p$  is some integer multiple of  $\Delta_p$ .

For each boson in an occupied state  $\mathbf{a}$ , we choose to attempt three successive transitions to a neighbor in the direction of each component of the force, rather than a single transition to one of the seven neighboring states. Also, the shared non-local force per boson  $\mathbf{F}_{\mathbf{a}}$  does not change during a time step even though the occupancy of the state may change during a time step as all the bosons in the subsystem sequentially attempt a transition.

For the occupied momentum state  $\mathbf{a}$ , the relevant neighbor state in the direction  $\alpha \in \{x, y, z\}$  is  $\mathbf{a}'_{\alpha} \equiv \mathbf{a} + \text{sign}(\tau F_{\mathbf{a}, \alpha}) \tilde{\Delta}_p \hat{\mathbf{x}}_{\alpha}$ . (Most commonly the time step  $\tau$  is positive and the neighboring momentum state lies in the direction of the force.) The conditional transition probability for the transition  $\{N_{\mathbf{a}}, N_{\mathbf{a}'_{\alpha}}\} \xrightarrow{\tau} \{N_{\mathbf{a}} - 1, N_{\mathbf{a}'_{\alpha}} + 1\}$  may be split into even and odd terms,

$$\varphi(N_{\mathbf{a}} - 1, N_{\mathbf{a}'_{\alpha}} + 1; t | N_{\mathbf{a}}, N_{\mathbf{a}'_{\alpha}}; t - \tau) = \varphi_{\alpha}^{+}(\mathbf{a}) + \varphi_{\alpha}^{-}(\mathbf{a}), \quad (2.12)$$

where  $\varphi_{\alpha}^{\pm}(-\mathbf{a}) = \pm \varphi_{\alpha}^{\pm}(\mathbf{a})$ . The probability of not changing state is  $\varphi(N_{\mathbf{a}}, N_{\mathbf{a}'_{\alpha}}; t | N_{\mathbf{a}}, N_{\mathbf{a}'_{\alpha}}; t - \tau) = 1 - \varphi_{\alpha}^{+}(\mathbf{a}) - \varphi_{\alpha}^{-}(\mathbf{a})$ . With this and the above result Bayes' theorem reads

$$\begin{aligned} & 1 - \frac{\beta}{m} \text{sign}(\tau F_{\mathbf{a}, \alpha}) \tilde{\Delta}_p a_{\alpha} + \frac{\beta \tau}{m} F_{\mathbf{a}, \alpha} a_{\alpha} \\ &= \frac{\varphi_{\alpha}^{+}(\mathbf{a}) + \varphi_{\alpha}^{-}(\mathbf{a})}{\varphi_{\alpha}^{+}(-\mathbf{a}'_{\alpha}) + \varphi_{\alpha}^{-}(-\mathbf{a}'_{\alpha})} \\ &\approx \frac{\varphi_{\alpha}^{+}(\mathbf{a})}{\varphi_{\alpha}^{+}(\mathbf{a}'_{\alpha})} \left[ 1 + \frac{\varphi_{\alpha}^{-}(\mathbf{a})}{\varphi_{\alpha}^{+}(\mathbf{a})} + \frac{\varphi_{\alpha}^{-}(\mathbf{a}'_{\alpha})}{\varphi_{\alpha}^{+}(\mathbf{a}'_{\alpha})} \right]. \end{aligned} \quad (2.13)$$

Now assume that to leading order

$$\varphi_{\alpha}^{+}(\mathbf{a}'_{\alpha}) = \varphi_{\alpha}^{+}(\mathbf{a}) [1 + \tilde{\Delta}_p^2 b_{\alpha}], \quad (2.14)$$

and

$$\varphi_{\alpha}^{-}(\mathbf{a}'_{\alpha}) = \varphi_{\alpha}^{-}(\mathbf{a}) = \varphi_{\alpha}^{+}(\mathbf{a}) [\tau c_{\alpha} + \tilde{\Delta}_p d_{\alpha}]. \quad (2.15)$$

These give

$$\begin{aligned} & 1 - \frac{\beta}{m} \text{sign}(F_{\mathbf{a}, \alpha}) \tilde{\Delta}_p a_{\alpha} + \frac{\beta \tau}{m} F_{\mathbf{a}, \alpha} a_{\alpha} \\ &= [1 - \tilde{\Delta}_p^2 b_{\alpha}] \left[ 1 + 2\tau c_{\alpha} + 2\tilde{\Delta}_p d_{\alpha} \right] \\ &= 1 + 2\tau c_{\alpha} + 2\tilde{\Delta}_p d_{\alpha}, \end{aligned} \quad (2.16)$$

with second order terms neglected. Hence

$$c_\alpha = \frac{\beta}{2m} F_{\mathbf{a},\alpha} a_\alpha, \text{ and } d_\alpha = \frac{\beta}{2m} \text{sign}(\tau F_{\mathbf{a},\alpha}) a_\alpha. \quad (2.17)$$

(The sign of  $d_\alpha$  is corrected in § D. Fortunately, these odd terms are small compared to unity and the numerical results are little affected.) Both of these are odd in  $a_\alpha$ , as required.

The average change in kinetic energy due to the stochastic transition in the  $\alpha$  direction is

$$\begin{aligned} \langle \Delta_\alpha \mathcal{K} \rangle &= \frac{\text{sign}(\tau F_{\mathbf{a},\alpha}) \tilde{\Delta}_p a_\alpha}{m} \\ &\quad \times \wp(N_{\mathbf{a}} - 1, N_{\mathbf{a}'_\alpha} + 1; t | N_{\mathbf{a}}, N_{\mathbf{a}'_\alpha}; t - \tau) \\ &= \frac{\text{sign}(\tau F_{\mathbf{a},\alpha}) \tilde{\Delta}_p a_\alpha}{m} [\wp_\alpha^+(\mathbf{a}) + \wp_\alpha^-(\mathbf{a})] \\ &\approx \frac{\text{sign}(\tau F_{\mathbf{a},\alpha}) \tilde{\Delta}_p a_\alpha}{m} \wp_\alpha^+(\mathbf{a}), \end{aligned} \quad (2.18)$$

again to leading order. Since this must equal the negative of the change in potential energy in the  $\alpha$  direction,  $(\tau/m) F_{\mathbf{a},\alpha} a_\alpha$ , we obtain

$$\wp_\alpha^+(\mathbf{a}) = \frac{|\tau F_{\mathbf{a},\alpha}|}{\tilde{\Delta}_p}. \quad (2.19)$$

This must be positive and less than unity, which can be ensured by choosing  $\tilde{\Delta}_p = n_\alpha \Delta_p$ , where  $n_\alpha$  is a positive integer. Choose  $n_\alpha$  to be as small as possible, but no smaller. Practical experience with the finite-sized simulations reported below has shown unity to be sufficient,  $\tilde{\Delta}_p = \Delta_p$ . The smaller the time step the smaller  $\wp_\alpha^+(\mathbf{a})$  is and the more likely the boson is to remain in its current momentum state.

Requiring the cancelation of kinetic and potential energies on average ensures energy conservation and the constancy of the equilibrium probability distribution on the stochastic adiabatic trajectory. It means that on average the change in momentum of the bosons in the state is equal to the classical change in momentum due to the force acting on them. Hence we expect that that these stochastic equations of motion will go over to the classical deterministic equations of motion in the thermodynamic limit in the non-condensed regime.

### C. Dissipative Transition

The dissipative transitions act like a thermostat and provide a more direct mechanism for the change in occupancy of the momentum states and for the equilibration of the occupancy distribution. For this we first randomly choose a boson from the  $N$  bosons in the subsystem, say  $j$ . We then choose with probability in inverse proportion to the occupancy of its state whether or not this boson will attempt a transition. (Attempt a transition only if a random number uniformly distributed on the unit interval is less than  $1/N_{\mathbf{p}_j}$ .) This step is necessary so that all

occupied states are treated equally irrespective of their occupancy. Finally, if a transition for  $j$  is to be attempted we use the conditional transition probability that follows for the 27 near neighbor states  $\mathbf{a}'$  (including the original state  $\mathbf{a}$ ). Typically, this sequence of steps is repeated in a block of  $N$ . The block is performed typically once every 10 time steps, although less frequent attempts would probably suffice.

The irreversible form of Bayes' theorem is required,

$$\begin{aligned} \frac{\wp(N_{\mathbf{a}'} + 1, N_{\mathbf{a}} - 1 | N_{\mathbf{a}'}, N_{\mathbf{a}})}{\wp(N_{\mathbf{a}'}, N_{\mathbf{a}} | N_{\mathbf{a}'} + 1, N_{\mathbf{a}} - 1)} &= \frac{\wp(N_{\mathbf{a}'} + 1) \wp(N_{\mathbf{a}} - 1)}{\wp(N_{\mathbf{a}'}) \wp(N_{\mathbf{a}})} \\ &= e^{-\beta(a'^2 - a^2)/2m}. \end{aligned} \quad (2.20)$$

There is no time step involved in this. Now  $\mathbf{a}' = \mathbf{a} + \mathbf{s} \Delta_p$  and  $a'^2 - a^2 = 2\Delta_p \mathbf{s} \cdot \mathbf{a} + \Delta_p^2 s^2$ , where  $s_\alpha \in \{-1, 0, 1\}$ . In view of classical dissipative dynamics based on the second entropy (Attard 2012), the conditional transition probability for  $\mathbf{a} \xrightarrow{j} \mathbf{a}'$  has the form

$$\wp(\mathbf{a}' | \mathbf{a}) = \wp_0 + (\mathbf{a}' - \mathbf{a}) \cdot \mathbf{R}_p(\mathbf{a}) / \Delta_p^2. \quad (2.21)$$

Normalization gives  $\wp_0 = 1/27$  and

$$\mathbf{R}_p(\mathbf{a}) = \frac{-\Delta_p^2}{54mk_B T} \mathbf{a}. \quad (2.22)$$

It can be confirmed that with this Bayes' theorem is satisfied to quadratic order. This is just the quantized version of the classical drag force.

The heart of the dissipative part of the algorithm is to calculate  $\wp(\mathbf{a}' | \mathbf{a})$  for each of the 27 nearest neighbors (including  $\mathbf{a}$ ), and place these in some one-dimensional order. This divides the unit interval into subintervals of width equal to the respective transition probability. Next choose a random number uniformly distributed on the unit interval. The boson  $j$  is moved to the momentum state corresponding to the subinterval into which the random number falls. Obviously if this subinterval corresponds to the original state  $\mathbf{a}$ , then no transition is made. The procedure is repeated for a new randomly chosen boson. There is nothing to prevent a boson being chosen more than once in the current block, in which case it could make several transitions, while other bosons have not been chosen at all.

This random choice of  $N$  bosons for transition is not essential. It was used for the quantum fluid for the results below. In what is called the classical fluid, all  $N$  bosons were cycled through in sequential order for an attempted transition. This difference between the treatment of the two fluids is not expected to be significant. For the quantum fluid a transition was attempted with probability in inverse proportion to the occupancy of its state. For the classical fluid, a transition was always attempted irrespective of the occupancy of its momentum state. This difference is significant.

This quantum dissipative algorithm was tested for ideal bosons. It was found that for  $N = 1,000$ ,  $T^* = 0.60$ ,  $\rho^* = 0.80$ , it gave the ground state occupancy as

$\langle N_{000} \rangle = 22.8(9)$ , which can be compared to the exact result 38.9. The results for the excited states were better; for example the first excited state had  $\langle N_{001} \rangle = 10.9(2)$  compared to the exact 12.5. For  $N = 10,000$  and the same density and temperature, the algorithm gave  $\langle N_{000} \rangle = 35.1(38)$ , with the exact result in this case being 40.9. The first excited state was  $\langle N_{001} \rangle = 26.2(24)$ , compared with the exact 27.9. This dependence on system size for the ground state occupancy is acceptable for the present purposes.

### 1. Alternative Expansion

As an alternative, expand the right hand side as

$$\begin{aligned} & \frac{\wp(N_{\mathbf{a}'} + 1)\wp(N_{\mathbf{a}} - 1)}{\wp(N_{\mathbf{a}'})\wp(N_{\mathbf{a}})} \\ &= e^{-\beta(a'^2 - a^2)/2m} \\ &= 1 - \frac{\beta}{2m}(a'^2 - a^2) + \frac{\beta^2}{8m^2}(a'^2 - a^2)^2 + \mathcal{O}(\Delta_p^3). \end{aligned} \quad (2.23)$$

For the conditional transition probability use the expansion

$$\begin{aligned} & \wp(N_{\mathbf{a}'} + 1, N_{\mathbf{a}} - 1 | N_{\mathbf{a}'}, N_{\mathbf{a}}) \\ &= A(\mathbf{a}) + B(\mathbf{a})(a'^2 - a^2) + C(\mathbf{a})(a'^2 - a^2)^2 + \mathcal{O}(\Delta_p^3). \end{aligned} \quad (2.24)$$

It is straightforward to show that

$$A(\mathbf{a}) = \frac{1}{27} + \mathcal{O}(\Delta_p^2), \text{ and } B(\mathbf{a}) = \frac{-\beta}{108m} + \mathcal{O}(\Delta_p^2). \quad (2.25)$$

The coefficient  $C(\mathbf{a})$  can be set to zero and the expansion of the right hand side will remain satisfied at  $\mathcal{O}(\Delta_p^2)$ .

Results for ideal bosons ( $N = 1,000$ ,  $T = 0.60$ ,  $\rho = 0.80$ ) gave the ground state occupancy as  $\langle N_{000} \rangle = 38.0(8)$ , compared to the exact 38.9, and the first excited state occupancy as  $\langle N_{001} \rangle = 13.3(1)$ , compared to the exact 12.5. For  $N = 10,000$  the algorithm gave  $\langle N_{000} \rangle = 41.9(40)$ , compared to the exact 40.9, and  $\langle N_{001} \rangle = 28.4(9)$ , compared to the exact 27.9.

Although these results for ideal bosons are better than those obtained with the second entropy algorithm, preliminary results suggested that the latter was better for interacting bosons, as judged by the kinetic energy in the classical case. Also the second entropy approach has fundamental justification in the classical limit (Attard 2012a). For these reasons it is the second entropy algorithm that is used to obtain the results given below.

### D. Viscosity Time Correlation Function

The shear viscosity can be expressed as an integral of the momentum-moment time-correlation function (Attard 2012a Eq. (9.117)),

$$\eta_{\alpha\gamma}(t) = \frac{1}{2Vk_B T} \int_{-t}^t dt' \left\langle \dot{P}_{\alpha\gamma}^0(\mathbf{\Gamma}) \dot{P}_{\alpha\gamma}^0(\mathbf{\Gamma}(t' | \mathbf{\Gamma}, 0)) \right\rangle. \quad (2.26)$$

It was Onsager (1931) who originally gave the relationship between the transport coefficients and the time correlation functions. It is therefore somewhat puzzling that this is called a Green-Kubo expression (Green 1954, Kubo 1966). The first  $\alpha$ -moment of the  $\gamma$ -component of momentum is

$$P_{\alpha\gamma} = \sum_{j=1}^N q_{j,\alpha} p_{j\gamma}. \quad (2.27)$$

The classical adiabatic rate of change of momentum moment is

$$\dot{P}_{\alpha\gamma}^0 = \frac{1}{m} \sum_{j=1}^N p_{j\alpha} p_{j\gamma} + \sum_{j=1}^N q_{j\alpha} f_{j\gamma}. \quad (2.28)$$

This can be shown to be symmetric,  $\dot{P}_{\gamma\alpha}^0 = \dot{P}_{\alpha\gamma}^0$ .

In the occupancy picture we cannot distinguish individual bosons, and so we should replace here the classical force on individual bosons by the shared non-local force on the bosons in each momentum state. Arguably this is equivalent to using the adiabatic stochastic transition probability since on average the two are the same. Therefore, for the momentum state  $\mathbf{a}$ , define the shared non-local force per boson and the center of mass,

$$\mathbf{F}_{\mathbf{a}} \equiv \frac{1}{N_{\mathbf{a}}} \sum_{j \in \mathbf{a}} \mathbf{f}_j, \text{ and } \mathbf{Q}_{\mathbf{a}} \equiv \frac{1}{N_{\mathbf{a}}} \sum_{j \in \mathbf{a}} \mathbf{q}_j. \quad (2.29)$$

Also define the total force on the momentum state  $\mathbf{a}$  due to the state  $\mathbf{b}$  to be

$$\mathbf{F}_{\mathbf{ab}} = \sum_{j \in \mathbf{a}} \sum_{k \in \mathbf{b}} \mathbf{f}_{jk}, \quad (2.30)$$

where  $\mathbf{f}_{jk}$  is the classical force on boson  $j$  due to boson  $k$ . Note that  $\mathbf{F}_{\mathbf{a}} = N_{\mathbf{a}}^{-1} \sum_{\mathbf{b}} \mathbf{F}_{\mathbf{ab}}$ . According to Newton,  $\mathbf{F}_{\mathbf{ab}} = -\mathbf{F}_{\mathbf{ba}}$  and  $\mathbf{F}_{\mathbf{aa}} = \mathbf{0}$ . Using these the adiabatic rate of change of the first momentum moment dyadic in the condensed regime is

$$\begin{aligned} \underline{\dot{P}}^0 &= \frac{1}{m} \sum_{j=1}^N \mathbf{p}_j \mathbf{p}_j + \sum_{\mathbf{a}} N_{\mathbf{a}} \mathbf{Q}_{\mathbf{a}} \mathbf{F}_{\mathbf{a}} \\ &= \frac{1}{m} \sum_{j=1}^N \mathbf{p}_j \mathbf{p}_j + \sum_{\mathbf{a}} \mathbf{Q}_{\mathbf{a}} \sum_{\mathbf{b}} \mathbf{F}_{\mathbf{ab}} \\ &= \frac{1}{m} \sum_{j=1}^N \mathbf{p}_j \mathbf{p}_j + \frac{1}{2} \sum_{\mathbf{a}, \mathbf{b}} \mathbf{Q}_{\mathbf{ab}} \mathbf{F}_{\mathbf{ab}}, \end{aligned} \quad (2.31)$$

where  $\mathbf{Q}_{\mathbf{ab}} = \mathbf{Q}_{\mathbf{a}} - \mathbf{Q}_{\mathbf{b}}$ . For the shared non-local force,  $\mathbf{f}_j \Rightarrow \mathbf{F}_{\mathbf{p}_j}$ , which means that the transformation to the center of mass is exact because all the bosons in the state experience the same force,  $\sum_{j \in \mathbf{a}} \mathbf{q}_j \mathbf{f}_j = \sum_{j \in \mathbf{a}} \mathbf{q}_j \mathbf{F}_{\mathbf{a}} = N_{\mathbf{a}} \mathbf{Q}_{\mathbf{a}} \mathbf{F}_{\mathbf{a}}$ . In so far as the momentum state is non-local, there are no spatial correlations between the bosons in the state, and on average  $\mathbf{Q}_{\mathbf{a}} \approx \mathbf{0}$  (although the fluctuations in this are macroscopic). Similarly the shared

non-local force likely averages close to zero for highly occupied states (again with large fluctuations). These two properties doubtless contribute to the molecular origin of the vanishing of the viscosity for condensed bosons.

Numerical results indicate that this dyadic is symmetric on average, in the same sense that all off-diagonal components of the dyadic are equal on average. The standard deviation of the six off-diagonal components of the viscosity time function gives an estimate of the statistical error.

### III. RESULTS

In what follows what is defined as the classical fluid is treated with the same algorithm as the quantum fluid but as if the occupancy of the momentum state was unity. That is, the force on each boson was taken to be the actual local force rather than the shared non-local force, and the dissipative transition was always attempted for the chosen boson irrespective of the occupancy of its momentum state. The viscosity was calculated with the actual local force rather than the shared non-local force. However, the momenta were still quantized and the adiabatic transitions were still stochastic, just as in the quantum case.

We used the Lennard-Jones pair potential,

$$u(r) = 4\epsilon \left[ \frac{\sigma^{12}}{r^{12}} - \frac{\sigma^6}{r^6} \right]. \quad (3.1)$$

We set this to zero for  $r > 3.5\sigma$ . The molecular diameter for helium is  $\sigma_{\text{He}} = 0.2556 \text{ nm}$  and the well-depth is  $\epsilon_{\text{He}}/k_{\text{B}} = 10.22 \text{ J}$  (van Sciver 2012). The mass is  $m_{\text{He}} = 4.003 \times 1.66054 \times 10^{-27} \text{ Kg}$ .

The results below are presented in dimensionless form: the temperature is  $T^* = k_{\text{B}}T/\epsilon_{\text{He}}$ , the number density is  $\rho^* = \rho\sigma_{\text{He}}^3$ , the time step is  $\tau^* = \tau/t_{\text{He}}$ , the unit of time is  $t_{\text{He}} = \sqrt{m_{\text{He}}\sigma_{\text{He}}^2/\epsilon_{\text{He}}}$ , and the shear viscosity is  $\eta^* = \eta\sigma_{\text{He}}^3/\epsilon_{\text{He}}t_{\text{He}}$ .

A canonical system with  $N = 1,000$  Lennard-Jones atoms was simulated with the above quantum stochastic molecular dynamics algorithm. The time step was  $\tau^* = 2 \times 10^{-5}$ . A block of  $N$  dissipative transitions was attempted once every 10 time steps. For the classical liquid this combination consistently gave a kinetic energy 2–3% higher than the exact value. The present parameters were judged acceptable even though a smaller time step or more frequent dissipative transitions would have given more accurate results, albeit at the cost of longer simulation times or greater interference in the adiabatic evolution of the momentum moment. Averages were collected once every 75 time steps. The number of time steps in a run was  $10 \times 4,000 \times 75$ . A run took about 24 hours on a desk-top personal computer. Four runs were made at each thermodynamic point. The quoted statistical error is the larger of the error estimated from the fluctuations in 10 blocks of each run (averaged across

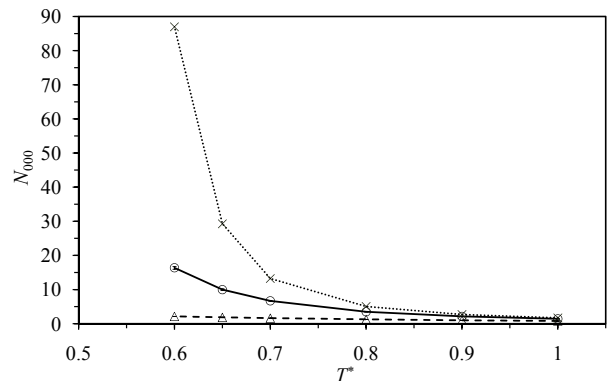


FIG. 2: Ground state occupancy in the saturated Lennard-Jones liquid. The circles are the quantum liquid, the triangles are the classical liquid, and the crosses are the exact result for ideal bosons. The error bars are less than the symbol size. The lines are an eye guide.

the runs), or the standard deviation across the four runs. There was usually little difference in the two estimates (but see below). The shear viscosity time function was estimated for  $t^* \leq 6$ , which meant that the time correlation function was covered ten times, and that  $4 \times 10 \times 6$  values were averaged at each time point for the quantum case, and  $4 \times 10 \times 3$  values in the classical case. The components of the quantized momentum were restricted to  $p_{j\alpha}^2/2mk_{\text{B}}T \leq 13$ .

The liquid saturation curve obtained in previous work was followed (Attard 2023a):  $\{T^*, \rho^*\} = \{1.00, 0.7009\}$ ,  $\{0.90, 0.7503\}$ ,  $\{0.80, 0.8023\}$ ,  $\{0.75, 0.8288\}$ ,  $\{0.70, 0.8470\}$ ,  $\{0.65, 0.8678\}$  and  $\{0.60, 0.8872\}$ .

Figure 2 shows the ground state occupancy on the saturation curve for the Lennard-Jones liquid. It can be seen that the present quantum molecular dynamics algorithm for the quantum liquid gives a larger occupancy than for the classical liquid, but smaller than that for ideal bosons. It has been argued that the ideal boson result should approximately apply to interacting bosons on the far side of the  $\lambda$ -transition (Attard 2025 §5.3). The smaller value evident in the figure could be due to finite size effects, or it could be due to forces in the interacting liquid pushing the ground state to neighboring momentum states, or it could be that the ideal boson model is a poor approximation for interacting bosons.

We defined a quantity `maxocc` to be the occupancy of the maximally occupied momentum state at each instant. For  $T^* = 0.65$ , `maxocc` = 22.3(2) for the quantum liquid, and 5.5773(4) for the classical liquid. (Here and throughout, the quantity in parentheses is the statistical error for the final digit or digits. It gives the 95% confidence level, as is also the case for the error bars in the figures.) The quantum result is close to the ideal boson result for the ground state occupancy,  $N_{000}^{\text{id}} = 29.3$ . However, at the higher temperature  $T^* = 0.90$ , `maxocc` = 9.71(3) in the quantum case, compared to  $N_{000}^{\text{id}} = 2.69$ . The ground

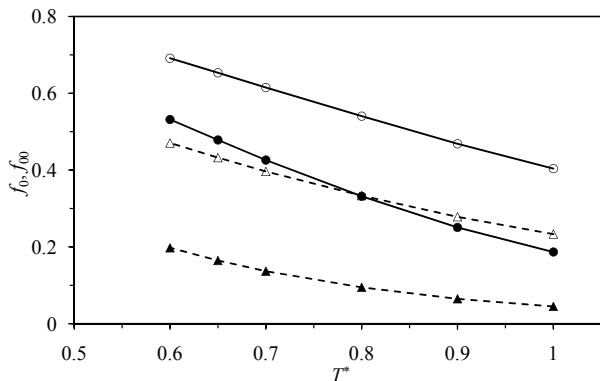


FIG. 3: Fraction of bosons condensed in the saturated Lennard-Jones liquid. The circles are the quantum liquid, the triangles are the classical liquid. The open symbols are  $f_0$ , the fraction in states occupied by two or more bosons, and the filled symbols are  $f_{00}$ , the fraction in states occupied by three or more bosons. The error bars are less than the symbol size. The lines are an eye guide.

state occupancy for the quantum liquid,  $N_{000}^{\text{qu}} = 2.14(3)$  is not too bad at this temperature.

In any case the occupancy of the ground state is clearly greater for the quantum liquid than for the classical liquid. However, the occupancy of the ground state in the quantum liquid is a small fraction of the total number of bosons in the subsystem. For example, the fraction of the subsystem in the ground state is 1% at  $T^* = 0.65$ . Obviously this means that ground state condensation cannot account for the  $\lambda$ -transition or for superfluidity.

Figure 3 gives the fraction of condensed bosons in the subsystem. Condensed bosons were defined as those in multiply occupied states, with a threshold set at 2 or 3. In the quantum liquid at the lowest temperature studied about 69% of the bosons are in states with two or more, and about 53% are in states with three or more. In contrast the fraction for the classical liquid is 47% and 20%, respectively. We can conclude that Bose-Einstein condensation is substantial, and that multiple momentum states are multiply occupied. That the majority of the bosons in the system can be considered to be condensed explains the macroscopic nature of the  $\lambda$ -transition and superfluidity.

It can be seen that at higher temperatures the condensation in the quantum liquid is approaching that in the classical liquid, as one would hope. However even at the highest temperature studied,  $T^* = 1$ , there is still excess condensation in the quantum liquid,  $f_0^{\text{qu}} = 40\%$  compared to  $f_0^{\text{cl}} = 23\%$ . That there remains condensation well-above the superfluid transition temperature is in part due to the neglect in the present calculations of position permutation loops, which suppress condensation (Attard 2025 §3.2). This has implications for the two-fluid model of superfluidity, which is discussed below.

The kinetic energy per boson in the classical liquid is  $\beta\mathcal{K}/N = 1.5406(6)$  at  $T^* = 0.90$  and  $1.5366(3)$  at  $T^* =$

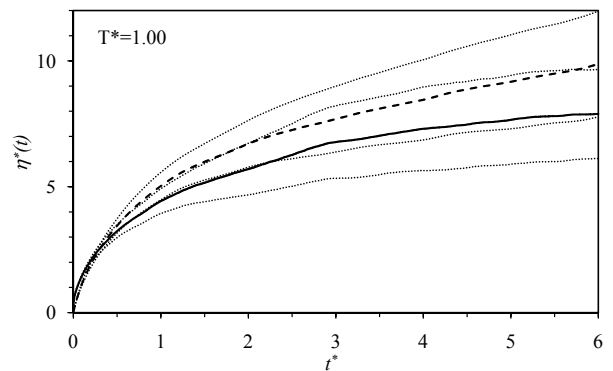


FIG. 4: Shear viscosity time function for the Lennard-Jones liquid at  $T^* = 1.00$  and  $\rho^* = 0.7009$ . The solid curve is the quantum liquid, the dashed curve is the classical liquid, and the dotted curves give the 95% confidence level.

0.60. The equipartition theorem gives the exact classical value as  $3/2$ . One can conclude that the present stochastic equations of motion that use the transition probability for quantized momentum are indeed going over to the classical equations of motion. The kinetic energy per boson in the quantum liquid is  $\beta\mathcal{K}/N = 1.2859(8)$  at  $T^* = 0.90$  and  $1.001(1)$  at  $T^* = 0.60$ . The decrease in kinetic energy with decreasing temperature is a manifestation of the increasing condensation in the quantum liquid that preferentially occurs in the low lying momentum states.

Figure 4 shows the shear viscosity time function for the quantum and classical liquids at the relatively high temperature of  $T^* = 1.00$ . The general features of the curves is that they rise from zero at  $t^* = 0$  to reach a maximum or a plateau, in this case at about  $t^* = 6$ . This maximum value is taken to be ‘the’ shear viscosity. It can be seen that the viscosity of the classical liquid is greater than that of the quantum liquid, although they do agree to within the statistical error over most of the time domain shown. The fraction of condensed bosons in states with two or more bosons at this temperature is 40% for the quantum liquid and 23% for the classical liquid (Fig. 3). Hence although one expects the quantum viscosity to go over to the classical viscosity as the temperature is increased, there still remains substantial Bose-Einstein condensation at this temperature.

The diffusion in the system was relatively small. The root mean square change in separation of a randomly chosen pair of bosons over the course of a run was  $0.91(32)$  for the quantum liquid and  $0.78(31)$  for the classical liquid. Nevertheless the statistical errors in the average potential energy and pressure were about the same whether estimated within a run or between runs. (Each run was started from an independently equilibrated configuration.) I conclude from this that the subsystem is liquid-like rather than glassy.

Figure 5 gives the shear viscosity time function at the lower temperature of  $T^* = 0.80$ . Note the change of



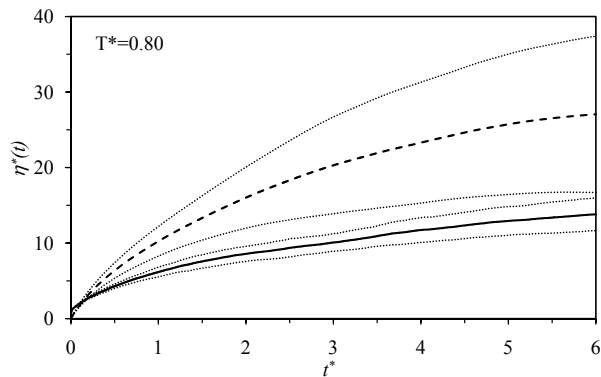


FIG. 5: As in the preceding figure but for  $T^* = 0.80$  and  $\rho^* = 0.8023$ .

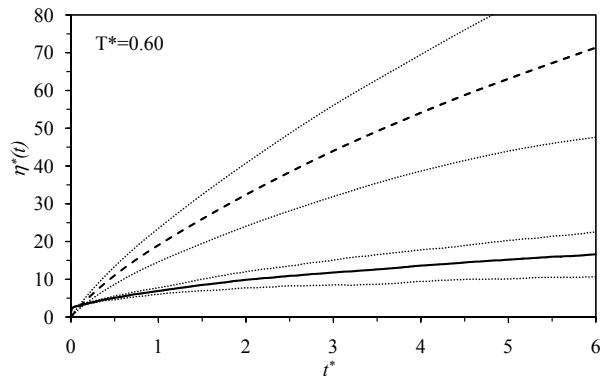


FIG. 6: As in the preceding figure but for  $T^* = 0.60$  and  $\rho^* = 0.8872$ .

scale. The viscosity of the quantum liquid is significantly lower than that of the classical liquid over virtually the whole domain. At very small times the quantum viscosity rises more quickly than the classical viscosity before flattening out. This effect was seen consistently in all the simulations, but the quantitative values in the small time regime appear sensitive to the frequency of the application of the dissipative thermostat (see below). The maximum viscosity of the classical liquid is much greater at this temperature than that at the higher temperature of the preceding figure. The root mean square change in separation was 0.54(16) for the quantum liquid and 0.43(7) for the classical liquid. The statistical errors in the average potential energy and pressure were a little smaller when estimated within a run than when estimated from between runs. I conclude from this that the subsystem is a little glassy.

Figure 5 shows the viscosity for the lowest temperature studied,  $T^* = 0.60$ . Note the change of scale again. It can be seen that the classical viscosity is substantially larger than the quantum viscosity everywhere except at very short times. The root mean square change in separation was 0.45(14) for the quantum liquid and 0.23(7) for the classical liquid. The statistical errors in the average potential energy and pressure were smaller when estimated

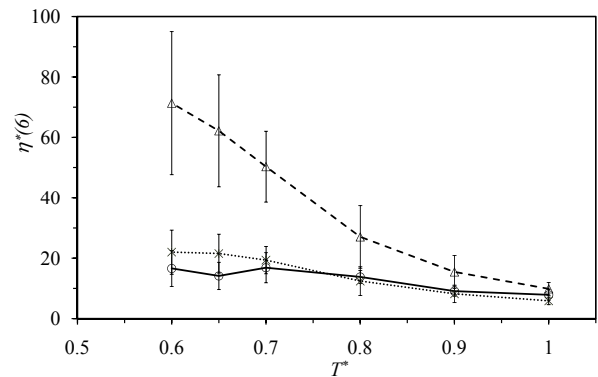


FIG. 7: Shear viscosity at  $t^* = 6$  on the Lennard-Jones liquid saturation curve. The circles and solid lines are for the quantum liquid  $\eta^{\text{qu}}$ , the triangles and dashed lines are for the classical liquid  $\eta^{\text{cl}}$ , and the asterisks and dotted lines are  $(1 - f_0^{\text{qu}})\eta^{\text{cl}}$ . The error bars give the 95% confidence level, and the lines are an eye guide.

within a run than when estimated from between runs, more noticeably so in the quantum case. I conclude from this that the subsystem is somewhat glassy. If this is the case then it is remarkable that the shear viscosity has a finite value, and that it is so low for the quantum liquid.

The results in this paper are based on the computer algorithm described above. Specifically, that the adiabatic transition for the quantum liquid used the shared non-local force, and that the bosons in each momentum state attempted a transition independently one at a time. An alternative is the so-called rigid body model in which the bosons in a momentum state are tied together so that either all or none make the adiabatic transition each time (Attard 2025). The formula for the shear viscosity is the same in both models. The two models should give the same result on average, but, from the fundamental point of view the present one at a time model is arguably preferable because it allows the adiabatic break-up of an occupied state. For the present case of  $T^* = 0.60$  and  $\rho^* = 0.8872$ , the present shared non-local force one at a time model gives  $\eta^*(6) = 16.6(59)$ , whereas the rigid body all or nothing model gives  $\eta^*(6) = 16.3(75)$ .

The present results applied the dissipative block once every 10 time steps, whereas the rigid body results just mentioned applied it once every 5 times steps. Reducing the frequency to once every 25 time steps, (and using runs nearly twice as long) the rigid body model gives  $\eta^*(6) = 19.0(28)$ . This is unchanged within the statistical error (although the statistical error itself appears smaller for less frequent applications of the dissipative transition). On very short time scales,  $t^* \lesssim 0.2$ , reducing the frequency of the dissipative transitions causes the viscosity to rise more quickly before flattening out.

Figure 7 shows the shear viscosity at  $t^* = 6$  as a function of temperature for the saturated liquid. Based on the extrapolation of fitted quadratics, the viscosity evaluated at this time is relatively close to the maximum

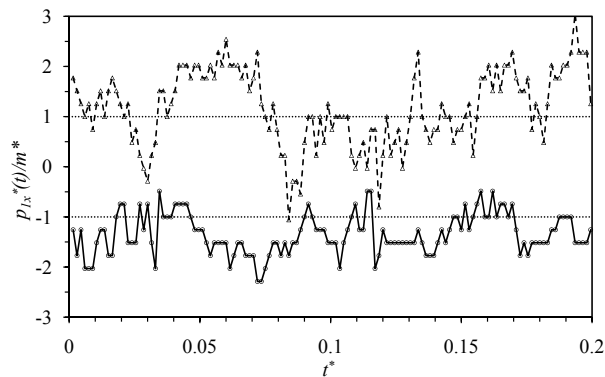


FIG. 8: Component of momentum of a typical boson on a trajectory at  $T^* = 0.60$  and  $\rho^* = 0.8872$ , plotted once every 75 time steps. The circles connected by solid lines are for the quantum liquid (offset by  $-1$ ) and the triangles connected by dashed lines are for the classical liquid (offset by  $+1$ ). The dotted lines are eye guides and the dimensionless spacing between momentum states is 0.26.

value of the viscosity in almost all cases. It can be seen that at higher temperatures the classical and quantum viscosities converge. At the lowest temperature studied the classical viscosity is about 4.5 times larger than the quantum viscosity. Whereas the classical viscosity increases markedly with decreasing temperature, the quantum viscosity is practically constant. This means that the increase in condensation with decreasing temperature in the quantum liquid, Fig. 3, increases the importance of the shared non-local force, and that this reduces the overall shear viscosity to the extent of overcoming the increasing glassiness of the subsystem.

The figure also includes results for  $(1 - f_0^{\text{qu}})\eta^{\text{cl}}(6)$ . This viscosity is the analogue of the two-fluid model of superfluidity (Landau 1941, Tisza 1938), namely it is the fraction of uncondensed bosons (ie. those in singly-occupied momentum states) in the quantum liquid times the viscosity in the classical liquid (ie. the viscosity calculated as if all the bosons were in singly-occupied momentum states). We would expect it to have some validity if the viscosity of condensed bosons is zero, and if the actual viscosity is a linear combination of that of the individual components of a two-component mixture. It can be seen that the two-fluid approximation is surprisingly good at lower temperatures. With increasing temperature the quantum and classical viscosities tend toward each other more quickly than the condensation goes to zero. This is the reason that the two-fluid ansatz underestimates the viscosity at the highest temperatures shown.

Of course the virtue of molecular dynamics simulations such as the present is that they enable the classical and quantum viscosities, as well as the distribution of occupancies, to be computed at any thermodynamic state point, and in molecular detail. One wonders how useful the two-fluid model really is, since it does not appear possible to actually measure the individual viscosities or the individual mole fractions in a laboratory.

Figure 8 shows a component of the momentum of a typical boson over time. It can be seen that there is a qualitative difference between the trajectory in the quantum liquid and in the classical liquid. The quantum equations of motion yield a smoother curve, with smaller fluctuations, and noticeable stretches of constant momentum. On this portion of the quantum trajectory, the occupancy of the momentum state that this boson is in ranges up to 26, and averages 5.20. The conclusion is that the shared non-local force in the quantum liquid damps the accelerations experienced by condensed bosons.

#### IV. CONCLUSION

The two-fluid model of superfluidity (Landau 1941, Tisza 1938) holds that below the  $\lambda$ -transition helium is a mixture of helium I and helium II, with the former having normal viscosity and the latter being the superfluid with zero viscosity. For a bulk measurement, the shear viscosity is believed to be a linear combination of the two in proportion to their mole fraction. Helium II is believed to consist of bosons condensed into the ground energy state.

I say that Bose-Einstein condensation occurs in the low-lying momentum states (Attard 2025). I also say that it is a simplification to divide the liquid into a mixture of two distinct fluids since there are multiple multiply-occupied states. Also, as few as two bosons in the same momentum state experience the effects permutation symmetry. Despite my disdain for the simplicity of the two-fluid model, I must concede that the results in Fig. 7 provide a measure of support for it, at least at low temperatures.

Elsewhere (Attard 2025 §5.3) I have argued that on the far side of the  $\lambda$ -transition  $^4\text{He}$  is dominated by momentum loops, which is to say permutations between bosons in the same momentum state. In this case the quantum statistical partition function factorizes into an ideal momentum part and a classical position configuration integral. This predicts that the occupancies of the momentum states are given by ideal statistics, for which the exact analytic results are known (Attard 2025 §2.2, Pathria 1972 §7.1). The present quantum stochastic molecular dynamics results tend to give a smaller occupancy for the ground momentum state, and also for excited momentum states, than that given by ideal statistics. It is possible that this is a finite size effect. Or else it says that interactions play a role in the occupancy and that the proposed factorization (Attard 2025 §5.3) is not entirely accurate. The arguments for the present shared non-local force model relied upon permutations between bosons in neighboring momentum states, not just between those in the same momentum state. In this sense the consequent dynamics are not fully compatible with the factorization model. This matter remains to be clarified.

Although this paper has focussed on the formulation of a computational algorithm for the viscosity of a quan-

tum liquid, it should not be assumed that the molecular equations of motion that are given are merely a numerical technique. The equations of motion yield real trajectories for particles, and there is reason to suppose that expressed in terms of transition probabilities they reflect the underlying reality of nature. This of course has implications for the physical interpretation of quantum mechanics. To which end I suggest

speculate, calculate, and mensurate. (4.1)

### References

- Attard P 2012a *Non-equilibrium thermodynamics and statistical mechanics: Foundations and applications* (Oxford: Oxford University Press)
- Attard P 2018 Quantum statistical mechanics in classical phase space. Expressions for the multi-particle density, the average energy, and the virial pressure arXiv:1811.00730
- Attard P 2021 *Quantum Statistical Mechanics in Classical Phase Space* (Bristol: IOP Publishing)
- Attard P 2023a *Entropy beyond the Second Law: Thermodynamics and statistical mechanics for equilibrium, non-equilibrium, classical, and quantum systems* (Bristol: IOP Publishing, 2nd edition)
- Attard P 2023b Quantum stochastic molecular dynamics simulations of the viscosity of superfluid helium arXiv:2306.07538
- Attard P 2023d Hamilton's equations of motion from Schrödinger's equation arXiv:2309.03349
- Attard P 2025 *Understanding Bose-Einstein Condensation, Superfluidity, and High Temperature Superconductivity* (London: CRC Press)
- Bohm D 1952 A suggested interpretation of the quantum theory in terms of 'hidden' variables. I and II. *Phys. Rev.* **85** 166
- de Broglie L 1928 La nouvelle dynamique des quanta, in *Solvay p.* 105
- Caldeira A O and Leggett A J 1983 Quantum tunnelling in a dissipative system *Ann. Phys.* **149** 374
- Goldstein S 2024 Bohmian mechanics *The Stanford Encyclopedia of Philosophy* (Summer 2024 Edition), E N Zalta and U Nodelman (eds.) URL = <<https://plato.stanford.edu/archives/sum2024/entries/qm-bohm/>>
- Green M S 1954 Markoff random processes and the statistical mechanics of time-dependent phenomena. II. Irreversible processes in fluids. *J. Chem. Phys.* **23**, 298
- Joos E and Zeh H D 1985 The emergence of classical properties through interaction with the environment *Z. Phys. B* **59** 223
- Kubo R 1966 The fluctuation-dissipation theorem *Rep.*

*Prog. Phys.* **29** 255

- Landau L D 1941 Theory of the superfluidity of helium II *Phys. Rev.* **60** 356
- Mermin D 1989 What's wrong with this pillow *Physics Today* **42** 9
- Mermin D 2004 Could Feynman have said this *Physics Today* **57** 10
- Merzbacher E 1970 *Quantum Mechanics* 2nd edn (New York: Wiley)
- Messiah A 1961 *Quantum Mechanics* (Amsterdam: North-Holland volumes 1 and 2)
- Onsager L (1931) Reciprocal relations in irreversible processes. I. *Phys. Rev.* **37** 405. Reciprocal relations in irreversible processes. II. *Phys. Rev.* **38** 2265
- Pathria R K 1972 *Statistical Mechanics* (Oxford: Pergamon Press)
- Schlosshauer M 2005 Decoherence, the measurement problem, and interpretations of quantum mechanics arXiv:quant-ph/0312059v4
- van Sciver S W 2012 *Helium Cryogenics* (New York: Springer 2nd edition)
- Tisza L 1938 Transport phenomena in helium II *Nature* **141** 913
- Zurek W H 1991 Decoherence and the transition from quantum to classical *Phys. Today* **44** 36
- Zurek W H, Cucchietti F M, and Paz J P 2003 Gaussian decoherence from random spin environments arXiv:quant-ph/0312207.

### Appendix A: Occupation of energy states?

The text invoked the occupation of low-lying momentum states. This contrasts with the conventional understanding of Bose-Einstein condensation, which maintains that condensation occurs into the ground energy state. This appendix proves that for interacting bosons the occupation of energy states is undefined.

Consider a system of  $N$  interacting bosons, which, for simplicity, has just two energy states with energy per boson  $e_1$  and  $e_2$ . If the occupancy picture is valid then the energy eigenvalues are of the form  $E = N_1 e_1 + N_2 e_2$ , where  $N_a$  is the number of bosons in state  $a$ . The energies per boson,  $e_1$  and  $e_2$ , must be independent of occupancy.

If we add an extra boson and place it in the first state,  $N \Rightarrow N + 1$ ,  $N_1 \Rightarrow N_1 + 1$ , then the second state must be unaffected. This implies that the eigenfunction of the second state must be independent of the new particle and its position. Hence the energy eigenfunction must factorize into those of the two states,

$$\phi_{N_1, N_2}(\mathbf{q}^{N_1}, \mathbf{q}^{N_2}) = \phi_{1, N_1}(\mathbf{q}^{N_1}) \phi_{2, N_2}(\mathbf{q}^{N_2}). \quad (\text{A.1})$$

This implies the energy eigenvalue equations

$$\begin{aligned}\hat{\mathcal{H}}_{1;N_1}(\mathbf{q}^{N_1})\phi_{1;N_1}(\mathbf{q}^{N_1}) &= N_1 e_1 \phi_{1;N_1}(\mathbf{q}^{N_1}) \\ \hat{\mathcal{H}}_{2;N_2}(\mathbf{q}^{N_2})\phi_{2;N_2}(\mathbf{q}^{N_2}) &= N_2 e_2 \phi_{2;N_2}(\mathbf{q}^{N_2}).\end{aligned}\quad (\text{A.2})$$

But these require the total Hamiltonian operator to be the sum of the individual Hamiltonian operators

$$\hat{\mathcal{H}}(\mathbf{q}^N) = \hat{\mathcal{H}}_{1;N_1}(\mathbf{q}^{N_1}) + \hat{\mathcal{H}}_{2;N_2}(\mathbf{q}^{N_2}).\quad (\text{A.3})$$

The interaction potential energy precludes this,  $U(\mathbf{q}^N) \neq U(\mathbf{q}^{N_1}) + U(\mathbf{q}^{N_2})$ .

There is an alternative way to see why factorization is forbidden by interaction. Using an abbreviated notation and assuming a factorized eigenfunction the energy eigenvalue equation is

$$\hat{\mathcal{H}}(\mathbf{q}_1, \mathbf{q}_2)\phi_1(\mathbf{q}_1)\phi_2(\mathbf{q}_2) = [E_1 + E_2]\phi_1(\mathbf{q}_1)\phi_2(\mathbf{q}_2),\quad (\text{A.4})$$

or

$$\frac{\hat{\mathcal{K}}(\mathbf{q}_1)\phi_1(\mathbf{q}_1)}{\phi_1(\mathbf{q}_1)} + \frac{\hat{\mathcal{K}}(\mathbf{q}_2)\phi_2(\mathbf{q}_2)}{\phi_2(\mathbf{q}_2)} + U(\mathbf{q}_1, \mathbf{q}_2) = E_1 + E_2.\quad (\text{A.5})$$

This follows since the kinetic energy operator is the sum of single-particle operators. Adding and subtracting this equation for states  $\mathbf{q}'_1$  and  $\mathbf{q}'_2$  gives

$$U(\mathbf{q}_1, \mathbf{q}_2) - U(\mathbf{q}'_1, \mathbf{q}_2) - U(\mathbf{q}_1, \mathbf{q}'_2) + U(\mathbf{q}'_1, \mathbf{q}'_2) = 0.\quad (\text{A.6})$$

But for nearby states this is just the second cross derivative of the potential,  $(\mathbf{q}'_2 - \mathbf{q}_2)(\mathbf{q}'_1 - \mathbf{q}_1) : \nabla_1 \nabla_2 U(\mathbf{q}_1, \mathbf{q}_2)$ . By definition this is non-zero for interacting particles. This proves that a factorized energy eigenfunction can only hold for non-interacting particles.

We conclude that it is meaningless to speak of the occupation of energy states for interacting particles.

## Appendix B: Momentum eigenfunctions

In the text, and indeed in all of our work on quantum statistical mechanics from the beginning (Attard 2018, 2021), we take the momentum eigenfunctions to be (normalized, unsymmetrized)

$$\phi_{\mathbf{p}}(\mathbf{q}) = \frac{1}{V^{N/2}} e^{-\mathbf{q} \cdot \mathbf{p} / i\hbar}.\quad (\text{B.1})$$

The spacing between momentum states is  $\Delta_p = 2\pi\hbar/L$ , where  $L$  is the edge length of the cubic subsystem, the volume being  $V = L^3$ , and there are  $N$  bosons in the subsystem. Where does this come from?

It is clear that this is an eigenfunction of the momentum operator,  $\hat{\mathbf{p}} = -i\hbar\nabla_{\mathbf{q}}$ . It is also clear that this is periodic,  $\phi_{\mathbf{p}}(\mathbf{q} + L\hat{\mathbf{x}}_{j\alpha}) = \phi_{\mathbf{p}}(\mathbf{q})$ . But this on its own is a little strange because the physical system being dealt with does not consist of a set of periodic replicas of the subsystem. One would have guessed that the boundary

condition should instead be that the wave function vanished on the boundary of the subsystem.

The reason for this form is that it ensures that the momentum operator is Hermitian, which is a fundamental requirement of quantum mechanics for an operator that represents a physical observable (Merzbacher 1970 Messiah 1961). To see this note that for periodic wave functions,

$$\begin{aligned}\int_V d\mathbf{q} \psi_1(\mathbf{q})^* \hat{\mathbf{p}} \psi_2(\mathbf{q}) &= -i\hbar \psi_1(\mathbf{q})^* \psi_2(\mathbf{q}) \Big|_{-L/2}^{L/2} \\ &\quad + i\hbar \int_V d\mathbf{q} (\nabla_{\mathbf{q}} \psi_1(\mathbf{q})^*) \psi_2(\mathbf{q}) \\ &= \int_V d\mathbf{q} (\hat{\mathbf{p}} \psi_1(\mathbf{q}))^* \psi_2(\mathbf{q}) \\ &\equiv \int_V d\mathbf{q} \psi_1(\mathbf{q})^* \hat{\mathbf{p}}^\dagger \psi_2(\mathbf{q}).\end{aligned}\quad (\text{B.2})$$

The integrated part vanishes on the boundary because of the periodicity, for example  $\psi(-L/2, y_j, z_j) = \psi(L/2, y_j, z_j)$ . The momentum eigenfunctions above form a complete basis set for such periodic wave functions. This links the quantization of the momentum states, which holds for a finite sized system, to the Hermitian nature of the momentum operator.

## Appendix C: Second order transition probabilities

In the body of the text it was found that the dissipative transition probability that was given underestimated the occupation of the ground momentum state for ideal bosons. The relative error was smaller for larger systems, which suggests that it is a finite size effect. This appendix gives second order equations for both the adiabatic transition and the dissipative transition.

### a. Adiabatic transition

The average change in kinetic energy due to the  $N_{\mathbf{a}}$  bosons in the momentum state  $\mathbf{a}$  making a transition to the nearby state  $\mathbf{a}'_{\alpha} = \mathbf{a} + \text{sign}(F_{\mathbf{a},\alpha})\tilde{\Delta}_p \hat{\mathbf{x}}_{\alpha}$  is

$$\begin{aligned}\langle \Delta_{\alpha} \mathcal{K} \rangle &= \frac{N_{\mathbf{a}}[a_{\alpha}'^2 - a_{\alpha}^2]}{2m} \wp(\mathbf{a}'_{\alpha}, t + \tau | \mathbf{a}, t), \\ &= \frac{N_{\mathbf{a}}[2\text{sign}(F_{\mathbf{a},\alpha})\tilde{\Delta}_p a_{\alpha} + \tilde{\Delta}_p^2]}{2m} \wp_{\alpha}^+(\mathbf{a}).\end{aligned}\quad (\text{C.1})$$

Since this must equal  $(\tau N_{\mathbf{a}}/m)F_{\mathbf{a},\alpha}a_{\alpha}$  we obtain

$$\wp_{\alpha}^+(\mathbf{a}) = \frac{2\tau F_{\mathbf{a},\alpha} a_{\alpha}}{2\text{sign}(F_{\mathbf{a},\alpha})\tilde{\Delta}_p a_{\alpha} + \tilde{\Delta}_p^2}.\quad (\text{C.2})$$

In practice we found  $\tilde{\Delta}_p = \Delta_p$  sufficient. The expression for  $\wp_{\alpha}^-(\mathbf{a})$  given in the text is unchanged. Note that in the ground momentum state  $\mathbf{a} = \mathbf{0}$ , in which case there

is no change in potential energy and there is no adiabatic transition. Changes in ground state occupancy can occur by the dissipative transitions (see next).

The adiabatic transitions discussed below are for the rigid body model: all bosons in the momentum state share the non-local force and make the transition together. The bosons tied together in each rigid body remain unchanged over a sequence of adiabatic transitions. The make-up of each rigid body was determined anew from the occupancies for each cycle of dissipative transitions.

### b. Dissipative transition

For the dissipative transition, expanding the kinetic energy to quadratic order gives in the configuration picture for  $\mathbf{a} \xrightarrow{j} \mathbf{a}'$ ,

$$\frac{\wp_j(\mathbf{a}'|\mathbf{a})}{\wp_j(\mathbf{a}|\mathbf{a}')} = \frac{N_{\mathbf{a}'} + 1}{N_{\mathbf{a}}} \left[ 1 - \frac{\beta(a'^2 - a^2)}{2m} \right]. \quad (\text{C.3})$$

The prefactor comes from the occupation entropy. Hence

$$\wp_j(\mathbf{a}'|\mathbf{a}) = \begin{cases} \frac{\varepsilon}{N_{\mathbf{a}}} \left[ 1 - \frac{\beta(a'^2 - a^2)}{4m} \right], & \mathbf{a}' \neq \mathbf{a} \\ 1 - \frac{26\varepsilon}{N_{\mathbf{a}}} + \frac{54\beta\Delta_p^2}{4m} \frac{\varepsilon}{N_{\mathbf{a}}}, & \mathbf{a}' = \mathbf{a}. \end{cases} \quad (\text{C.4})$$

For the following results,  $\varepsilon = 1/27$ . The dissipative transitions were attempted one boson at a time, for all  $N$  bosons in a cycle. A cycle of such attempts was made once every `skipcon` adiabatic time steps.

Note that in contrast to the occupation picture discussed in the text, the weighting inversely proportional to the occupancy is automatically built into this configuration picture; a transition attempt was made once for every boson in a cycle.

### c. Results

For ideal bosons, the second order dissipative transition algorithm for  $T = 0.60$ ,  $\rho = 0.8872$ , and  $N = 1,000$ , gave for the occupancies of the first several low lying momentum states:  $N_{000} = 85.9(43)$ , (exact is 87.0),  $N_{001} = 16.1(3)$ , (exact is 14.5),  $N_{011} = 8.2(1)$ , (exact is 7.73),  $N_{111} = 5.39(4)$ , (exact is 5.17),  $N_{002} = 3.94(3)$ , (exact is 3.83).

For  $T = 0.60$ ,  $\rho = 0.8872$ , and  $N = 10,000$ , the results were  $N_{000} = 138.2(284)$ , (exact is 138.0),  $N_{001} = 52.0(31)$ , (exact is 51.9),  $N_{011} = 33.3(8)$ , (exact is 31.8),  $N_{111} = 23.5(5)$ , (exact is 22.8),  $N_{002} = 18.3(6)$ , (exact is 17.8). It can be seen that these improve significantly the results of linear algorithm given in the text.

Table I shows results for the second order algorithm varying the frequency of the dissipative transitions. The rigid body model of shared non-local force was used,

TABLE I: Second order quantum molecular dynamics results for saturated Lennard-Jones  $\text{He}^4$  at  $T^* = 0.60$ ,  $\rho^* = 0.8872$ , and  $N = 1,000$ . `skipcon` is the number of adiabatic time steps between each cycle of stochastic dissipative transitions. The ground state occupancy for ideal bosons is  $N_{000}^{\text{id}} = 86.97$ .

<code>skipcon</code>	$\beta U/N$	$N_{000}$	$f_0$	$\eta^*(6)$
1	-10.19(2)	88.0(24)	0.7388(1)	30.3(86)
2	-10.18(2)	89.1(46)	0.7384(2)	21.5(76)
5	-10.165(9)	93.4(49)	0.7365(2)	25.0(62)
10	-10.17(1)	131.5(132)	0.7377(7)	20.8(81)
10 <sup>a</sup>	-10.04(2)	71.1(29)	0.7454(2)	22.9(52)

<sup>a</sup> $N = 500$ ,  $N_{000}^{\text{id}} = 65.11$ .

which is to say that the bosons in a momentum state evolved together, and that these ties were conserved over the adiabatic part of the trajectory. The ties were recalculated for the current occupancies for each cycle of dissipative transitions. It can be seen that when the dissipative transitions are applied most frequently, `skipcon`  $\lesssim 5$ , the ground state occupancy is close to that of ideal bosons. At `skipcon` = 10, the ground state occupancy is significantly greater than that of ideal bosons. In contrast, the fraction of condensed bosons,  $f_0$ , is much less sensitive to the frequency of the dissipative transitions. That the shear viscosity is similarly insensitive shows that it is dependent upon the amount of condensation rather than the number of bosons in the ground momentum state. This in turn means that errors in the ground state occupancy have little effect on the shear viscosity.

The viscosity was significantly higher for the most frequent application of the dissipative transition, `skipcon` = 1. The dissipative transitions should be regarded as a perturbation of the adiabatic motion, which requirement should be balanced with the need to obtain the correct occupancy distribution.

Compared to the first order, one-at-a-time algorithm discussed in the text, this second order rigid body algorithm gives a significantly higher ground state occupancy. The fraction of condensed bosons and the shear viscosity are comparable in the two. It augers well for the quantum dynamics that these quantities are robust.

Table I also shows results for a smaller system,  $N = 500$ . Although the results are not quite fully equilibrated, they confirm that within the statistical error the shear viscosity is independent of the system size.

We did a test for the rigid body model using the linear adiabatic transitions of the text combined with the quadratic dissipative transitions of this appendix. For `skipcon` = 10, we found  $N_{000} = 31.2(23)$  (compared with  $N_{000}^{\text{id}} = 86.97$ ),  $f_0 = 0.7175(3)$ , and  $\eta^*(6) = 16.9(38)$ . The ground state occupancy and condensation are significantly smaller than those given by the quadratic adiabatic transitions. The linear adiabatic equations have a non-zero probability for bosons in the ground momentum state to make a transition to an excited state, whereas for

the quadratic adiabatic equations the transition probability is zero. Combining the linear and quadratic forms is difficult to justify.

We also tested the shared non-local force but with one-at-a-time adiabatic transitions, again using the second order equations for both the adiabatic and dissipative transitions. For `skipcon` = 5, the ground state occupancy was  $N_{000} = 315.6(162)$  compared to  $N_{000}^{\text{id}} = 86.97$ . Thus the one-at-a-time algorithm gives a ground momentum state occupancy that is about 3.5 times the ideal boson result. Conversely, the first excited state is about half the ideal value:  $N_{001} = 7.6(5)$  compared to  $N_{001}^{\text{id}} = 14.53$ . The shared local force applied all-together (rigid body) for the same parameters gave  $N_{000} = 93.4(49)$  and  $N_{001} = 15.2(3)$ . We conclude that the one-at-a-time adiabatic algorithm is not viable and that the adiabatic transition has to apply to the occupied momentum state as a whole. Also, the rigid body (ie. the bosons tied initially together) has to be conserved over the adiabatic part of the trajectory, so that the occupancy is only recalculated at each dissipative transition.

Two general conclusions can be drawn from the results in this appendix. Attard (2025 §5.3) showed that on the far side of the  $\lambda$ -transition the partition function exactly factorized into an ideal boson momentum configuration integral and an interacting boson classical position configuration integral. This assumed that pure momentum permutation loops dominated, and that the commutation function was negligible. This purely static result says that the ideal boson momentum state occupancy is exact for interacting bosons on the far side of the  $\lambda$ -transition. The fact that the present rigid body quadratic transitions also give the ideal boson occupancy distribution confirms these as the appropriate molecular dynamics for interacting bosons in the condensed regime. The second, related, point is that the rigid body, shared non-local force formulation with ties conserved preserves the occupation entropy and hence the probability distribution on the adiabatic trajectory. This is consistent with general statistical principles for an equilibrium system (Attard 2012a Ch. 7), and with the particular thermodynamic principle for superfluidity deduced empirically from the measured fountain pressure (Attard 2025 Ch. 4).

#### Appendix D: Corrected Adiabatic Transition

The quantity  $d_\alpha$  has the wrong sign in Eq. (2.17) and in the subsequent numerical results in §§ III and C 0c. Fortunately, this has only a minor effect on the fraction of condensed bosons and on the viscosity.

The odd probability should be

$$\wp_\alpha^-(\mathbf{a}) = \wp_\alpha^+(\mathbf{a}) \left[ \tau \frac{\beta N_{\mathbf{a}}}{2m} F_{\mathbf{a},\alpha} a_\alpha - \Delta_p \frac{\beta N_{\mathbf{a}}}{2m} \text{sign}(\tau F_{\mathbf{a},\alpha}) a_\alpha \right]. \quad (\text{D.1})$$

This guarantees microscopic reversibility for any even function  $\wp_\alpha^+(\mathbf{a})$ . An explicit expression for the latter fol-

TABLE II: Size dependence of fractional occupancy at  $T^* = 0.60$ ,  $\rho^* = 0.8872$  using the present adiabatic transition, Eq. (D.5), and quadratic dissipative transition, Eq. (C.4), once every 10 time steps.

N	$f_{000}^{\text{id}}$	$f_{000}$	$f_0$
500	0.13023	0.26(1)	0.7659(6)
1000	0.08697	0.295(9)	0.7629(6)
2000	0.05446	0.352(14)	0.7652(9)
5000	0.02607	0.436(21)	0.7749(11)

lows by demanding that to leading order the average rate of change of momentum equal the shared non-local force,

$$N_{\mathbf{a}} F_{\mathbf{a},\alpha} = \frac{1}{\tau} N_{\mathbf{a}} \text{sign}(\tau F_{\mathbf{a},\alpha}) \Delta_p \wp_\alpha^+(\mathbf{a}). \quad (\text{D.2})$$

This is the quantum analogue of Newton's second law of motion. Hence we expect that that these stochastic equations of motion will go over to the classical deterministic equations of motion in the thermodynamic limit in the non-condensed regime. Rearranging this gives the even part of the conditional transition probability as

$$\wp_\alpha^+(\mathbf{a}) = \frac{|\tau F_{\mathbf{a},\alpha}|}{\Delta_p}. \quad (\text{D.3})$$

Note that this is strictly even in momentum, as it has to be, whereas the quadratic adiabatic form given and used in the preceding appendix is not. This is the justification for combining the present linear adiabatic result with the quadratic dissipative result, Eq. (C.4).

With this and the odd term, the average change in energy per boson due to the motion of bosons in the momentum state  $\mathbf{a}$  in the direction  $\alpha$  over a time step is

$$\begin{aligned} & \langle \Delta_{\mathbf{a},\alpha} \mathcal{H} \rangle / N_{\mathbf{a}} \quad (\text{D.4}) \\ &= \frac{-\tau}{m} F_{\mathbf{a},\alpha} a_\alpha + \frac{|\tau F_{\mathbf{a},\alpha}|}{\Delta_p} \left[ 1 + \tau \frac{N_{\mathbf{a}} \beta F_{\mathbf{a},\alpha} a_\alpha}{2m} \right. \\ & \quad \left. - \Delta_p \frac{N_{\mathbf{a}} \text{sign}(\tau F_{\mathbf{a},\alpha}) \beta a_\alpha}{2m} \right] \frac{a_\alpha'^2 - a^2}{2m} \\ &= \frac{|\tau F_{\mathbf{a},\alpha}| \Delta_p}{2m} + \frac{\tau^2 N_{\mathbf{a}} \beta (F_{\mathbf{a},\alpha} a_\alpha)^2}{2m^2} - \frac{\beta N_{\mathbf{a}} \Delta_p |\tau F_{\mathbf{a},\alpha}| a_\alpha^2}{2m^2}. \end{aligned}$$

This is second order since the linear contribution has canceled.

Putting these results together, the conditional transition probability in the  $\alpha$  direction is explicitly

$$\wp(\mathbf{a}'_\alpha | \mathbf{a}; \tau) = \frac{|\tau F_{\mathbf{a},\alpha}|}{\Delta_p} \left\{ 1 + \frac{\tau \beta N_{\mathbf{a}}}{2m} F_{\mathbf{a},\alpha} a_\alpha - \frac{\beta \Delta_p N_{\mathbf{a}}}{2m} \text{sign}(\tau F_{\mathbf{a},\alpha}) a_\alpha \right\}, \quad (\text{D.5})$$

where  $\mathbf{a}'_\alpha = \mathbf{a} + \text{sign}(\tau F_{\mathbf{a},\alpha}) \Delta_p$ . Since there is only a single transition state, the probability of not making the

transition is  $\wp(\mathbf{a}|\mathbf{a}; \tau) = 1 - \wp(\mathbf{a}'_\alpha|\mathbf{a}; \tau)$ . The smaller the time step the smaller  $\wp_\alpha^+(\mathbf{a})$  is and the more likely the bosons are to remain in the current momentum state in the current time step.

Table II gives results at the lowest temperature studied for the fractional occupancy as a function of system size. It can be seen that the ground state occupancy is in poor agreement with the ideal boson result, and it gets worse as the system size is increased. In contrast, the fraction of condensed bosons is remarkably insensitive to the system size. The condensed fraction  $f_0 = 0.7629(6)$  is not so different to that in the text  $f_0 = 0.6912(3)$  (Fig. 3) or in the preceding appendix  $f_0 = 0.7377(7)$  (Table I), both of which have the wrong sign for  $d_\alpha$ .

The viscosity for  $N = 1,000$  was  $\eta^*(6) = 22.9(42)$ , which is to be compared to the estimate  $\eta^*(6) = 16.6(59)$  (Fig. 6) and  $\eta^*(6) = 20.8(81)$  (Table I). It can be concluded that the viscosity depends much more upon the condensation fraction rather than the occupancy of the ground momentum state. Nevertheless the failure of the present algorithm to reliably give the ground state occupancy calls for further speculation, calculation, and mensuration.

### Appendix E: Configurational Adiabatic Transition

A deficiency with the rigid body adiabatic approach is that it on its own it does not allow the occupancies to change. Of course it does allow the specific states that are occupied to change, and in the dissipative step the occupancies do change. In the rigid body algorithm bosons that are in the same momentum state at the start of a adiabatic trajectory remain tied together as a rigid body sharing the same non-local force even as it evolves. This remains the case even when two such rigid bodies move into the same momentum state and transition independently out of it. This requirement is somewhat artificial and arbitrary, although it is motivated by the need to preserve the occupation entropy on the adiabatic trajectory.

An arguably better approach is to apply the shared non-local forces to independent subsets of the bosons in an occupied momentum state at each adiabatic time step. This raises the question of how to select the subsets in a statistically appropriate fashion.

The approach taken here is based on the fact that each permutation of the bosons in a momentum state is equally likely. Therefore at each time step a random permutation of the bosons in the state can be made, and each of the permutation loops it comprises can be taken as a subset for the transition. This may be called the rigid subset model.

A simple algorithm to generate a random permutation is as follows. For the  $N_{\mathbf{a}}$  bosons in the momentum state  $\mathbf{a}$ , create a pointer vector with entries  $v_j = j$ ,  $j = 1, 2, \dots, N_{\mathbf{a}}$ . Uniformly and randomly choose an element and place it at the head of a second vector. Close up

the first vector so that it now has length  $N_{\mathbf{a}} - 1$ , randomly choose another element from this shortened first vector, and place it second in the second vector. Continue in this fashion until all  $N_{\mathbf{a}}$  elements have been chosen. Compare the second vector with the original first vector to identify the permutation loops, which can be taken to be the rigid subsets.

Unlike the rigid body model used in the text and in the previous appendices, which conserved the occupation entropy over the adiabatic part of the trajectory, the present rigid subset model allows the momentum state to break up and the bosons ties to rearrange according to the state that they occupy after each successful transition. This shifts from the occupancy picture to the configuration picture, and therefore changes in occupation entropy must be taken into account. The configuration probability density is

$$\wp(\mathbf{\Gamma}) = \frac{1}{Z} e^{-\beta\mathcal{K}(\mathbf{p})} e^{-\beta U(\mathbf{q})} \prod_{\mathbf{a}} N_{\mathbf{a}}!, \quad (\text{E.1})$$

where the occupancy of the momentum state  $\mathbf{a}$  is  $N_{\mathbf{a}} = \sum_{j=1}^N \delta_{\mathbf{p}_j, \mathbf{a}}$ . Here a point in quantized phase space is  $\mathbf{\Gamma} = \{\mathbf{q}, \mathbf{p}\}$ . The conjugate point with momenta reversed is  $\mathbf{\Gamma}^\dagger = \{\mathbf{q}, -\mathbf{p}\}$ .

Consider the transition of a single subset  $A$  with  $n_A$  specific bosons from  $\mathbf{a}$  to  $\mathbf{a}'_\alpha = \mathbf{a} + \text{sign}(\tau F_{A,\alpha}) \Delta_p \hat{\mathbf{x}}_\alpha$ . Microscopic reversibility gives the ratio of conditional transition probabilities is

$$\begin{aligned} \frac{\wp(\mathbf{\Gamma}'|\mathbf{\Gamma}; \tau)}{\wp(\mathbf{\Gamma}^\dagger|\mathbf{\Gamma}'^\dagger; \tau)} &= \frac{\wp(\mathbf{\Gamma}')}{\wp(\mathbf{\Gamma})} \\ &= e^{(-n_A \beta / 2m)[a'^2 - a^2]} e^{(n_A \beta \tau / m) \mathbf{F}_{A,\alpha} \cdot \mathbf{a}} \\ &\quad \times \frac{(N_{\mathbf{a}'} + n_A)!(N_{\mathbf{a}} - n_A)!}{N_{\mathbf{a}'}! N_{\mathbf{a}}!}. \end{aligned} \quad (\text{E.2})$$

By inspection, this is satisfied by a conditional transition probability with the general form

$$\begin{aligned} \wp(\mathbf{a}'_\alpha|\mathbf{a}, n_A, N_{\mathbf{a}}, N_{\mathbf{a}'_\alpha}) & \quad (\text{E.3}) \\ &= \lambda_{A,\alpha} g(n_A) \left( \frac{(N_{\mathbf{a}'_\alpha} + n_A)!}{N_{\mathbf{a}'_\alpha}!} \right)^{1-r} \left( \frac{(N_{\mathbf{a}} - n_A)!}{N_{\mathbf{a}}!} \right)^r \\ &\quad \times \left\{ 1 - \frac{n_A \beta \Delta_p}{2m} \text{sign}(\tau F_{A,\alpha}) a_\alpha + \frac{n_A \beta \tau}{2m} F_{A,\alpha} a_\alpha \right\}. \end{aligned}$$

The exponential of the change in energy has been linearized here.

The two main cases of interest are  $r = 1$  and  $r = 1/2$ . These give the average rate of change of momentum in the direction  $\alpha$  for the subset  $A \in \mathbf{a}$  to leading order as

$$\begin{aligned} \langle \dot{p}_A^0 \rangle &= \frac{n_A}{\tau} \text{sign}(\tau F_{A,\alpha}) \Delta_p \lambda_{A,\alpha} g(n_A) \quad (\text{E.4}) \\ &\quad \times \begin{cases} \frac{(N_{\mathbf{a}} - n_A)!}{N_{\mathbf{a}}!}, & r = 1, \\ \sqrt{\frac{(N_{\mathbf{a}'_\alpha} + n_A)!(N_{\mathbf{a}} - n_A)!}{N_{\mathbf{a}'_\alpha}! N_{\mathbf{a}}!}}, & r = 1/2. \end{cases} \end{aligned}$$

TABLE III: Size dependence at  $T^* = 0.60$ ,  $\rho^* = 0.8872$  using rigid subset adiabatic transitions, Eqs (E.3) and (E.5) with  $r = 1$ , and quadratic dissipative transitions, Eq. (C.4), once every 10 time steps,  $\tau^* = 2 \times 10^{-5}$ .

N =	500		1,000		2,000		5,000	
	QMD	ideal	QMD	ideal	QMD	ideal	QMD	ideal
$f_{000}$	0.143(4)	0.13023	0.095(6)	0.08697	0.064(1)	0.05446	0.036(9)	0.02607
$f_{001}$	0.0209(4)	0.01848	0.0165(5)	0.01453	0.013(1)	0.01115	0.010(2)	0.00745
$f_{011}$	0.0102(1)	0.00954	0.0083(1)	0.00773	0.0067(2)	0.00611	0.0052(5)	0.00431
$f_{111}$	0.00647(4)	0.00625	0.00544(6)	0.00517	0.00436(8)	0.00417	0.0035(2)	0.00302
$f_{002}$	0.00465(3)	0.00454	0.00393(4)	0.00383	0.0032(1)	0.00313	0.0025(2)	0.00231
$f_0$	0.7520(2)	–	0.7434(2)	–	0.7388(4)	–	0.7366(4)	–
$\beta U/N$	-9.98(3)	–	-9.95(5)	–	-9.93(4)	–	-9.87(1)	–
$\eta^*(6)$	27.6(57)	–	32.6(75)	–	34.3(135)	–	64.6(496)	–

In the classical regime,  $N_{\mathbf{a}} = n_A = 1$  and  $N_{\mathbf{a}'_\alpha} = 0$ , these correspond to Newton's second law of motion when  $g(n_A) \equiv 1$  and

$$\lambda_{A,\alpha} \equiv \frac{|\tau F_{A,\alpha}|}{\Delta_p}. \quad (\text{E.5})$$

Moreover, when  $N_{\mathbf{a}'_\alpha} = N_{\mathbf{a}} - n_A$ , there is no change in occupation entropy over the transition and so in this case we also expect classical behavior. And indeed, for these choices of  $\lambda$  and  $g(n_A)$  we see that the second of these,  $r = 1/2$ , also satisfies Newton's second law. This is an argument in favor of  $r = 1/2$  (but see below).

More generally, Newton's second law is *not* satisfied in the quantum condensed regime. (As a consequence neither energy nor momentum are conserved, which is not unexpected as these results apply to an *open* quantum subsystem.) Specifically, the first of these,  $r = 1$ , says that for a highly occupied momentum state the rate of change of momentum is much less than the classical prediction for a given applied force. The second of these,  $r = 1/2$ , says similar for a transition from a highly occupied to a lowly occupied momentum state. In both cases the diminution factor is exponentially decreasing with subset size, being  $\mathcal{O}(N_{\mathbf{a}}^{-n_A})$  for the first and  $\mathcal{O}((N_{\mathbf{a}'_\alpha}/N_{\mathbf{a}})^{n_A/2})$  for the second. Typically,  $N_{\mathbf{a}} = \mathcal{O}(10^2)$ . Since superfluid flow consists selectively of bosons in highly occupied states, it is highly likely that  $N_{\mathbf{a}} \gg N_{\mathbf{a}'_\alpha}$ , and therefore that the rate of change of their momentum is exponentially reduced. It follows that there is a direct connection between the conservation of entropy on an adiabatic trajectory, the reduction in the rate of change of momentum in the condensed regime, and the loss of shear viscosity in superfluidity.

A second contribution to the reduction in the rate of change of momentum is the shared non-local force. That for the momentum state,  $n_A \mathbf{F}_{\mathbf{a}}$ , applied to the subset  $A \in \mathbf{a}$ , and that for the subset itself,  $n_A \mathbf{F}_A$ , which is the total force of the subset, can be used. Both lead to a cancelation of the local individual forces so that even classically the subset is less likely to change its momentum state than some of the individual bosons that comprise it. The sum of classical changes in the magnitude of

momentum components for bosons in a subset is greater than the magnitude of the classical change in momentum components of the rigid subset. The rigid body results in the text show that this is an important contribution to the reduction in viscosity in the condensed regime.

The viscosity can be calculated as in the text, § IID, but now in terms of rigid subsets. For a given configuration divided into permutation loops  $A = 1, 2, \dots$ , the shared non-local force per boson and the center of mass of a loop are

$$\mathbf{F}_A \equiv \frac{1}{n_A} \sum_{j \in A} \mathbf{f}_j, \text{ and } \mathbf{Q}_A \equiv \frac{1}{n_A} \sum_{j \in A} \mathbf{q}_j. \quad (\text{E.6})$$

(Here and below it is implicit that the loop  $A$  is a subset of a single momentum state; writing  $\sum_A$  is short for  $\sum_{\mathbf{a}} \sum_{A \in \mathbf{a}}$ .) The total force on the loop  $A$  due to the loop  $B$  is

$$\mathbf{F}_{AB} = \sum_{j \in A} \sum_{k \in B} \mathbf{f}_{jk}, \quad (\text{E.7})$$

where  $\mathbf{f}_{jk}$  is the classical force on boson  $j$  due to boson  $k$ . Note that  $\mathbf{F}_A = n_A^{-1} \sum_B \mathbf{F}_{AB}$ . According to that well-known reactionary Newton,  $\mathbf{F}_{AB} = -\mathbf{F}_{BA}$  and  $\mathbf{F}_{AA} = \mathbf{0}$ . With these, the adiabatic rate of change of the first momentum moment is for  $r = 1$

$$\begin{aligned} \underline{\dot{P}}^0 &= \frac{1}{m} \sum_{j=1}^N \mathbf{p}_j \mathbf{p}_j + \sum_A \sum_{j \in A} \mathbf{q}_j \frac{(N_{\mathbf{a}} - n_A)!}{N_{\mathbf{a}}!} \mathbf{F}_A \\ &= \frac{1}{m} \sum_{j=1}^N \mathbf{p}_j \mathbf{p}_j + \sum_A \frac{(N_{\mathbf{a}} - n_A)!}{N_{\mathbf{a}}!} n_A \mathbf{Q}_A \mathbf{F}_A \\ &= \frac{1}{m} \sum_{j=1}^N \mathbf{p}_j \mathbf{p}_j + \sum_A \frac{(N_{\mathbf{a}} - n_A)!}{N_{\mathbf{a}}!} \mathbf{Q}_A \sum_B \mathbf{F}_{AB} \\ &= \frac{1}{m} \sum_{j=1}^N \mathbf{p}_j \mathbf{p}_j + \frac{1}{2} \sum_{A,B} \tilde{\mathbf{Q}}_{AB} \mathbf{F}_{AB}, \end{aligned} \quad (\text{E.8})$$

where

$$\tilde{\mathbf{Q}}_{AB} \equiv \frac{(N_{\mathbf{a}} - n_A)!}{N_{\mathbf{a}}!} \mathbf{Q}_A - \frac{(N_{\mathbf{b}} - n_B)!}{N_{\mathbf{b}}!} \mathbf{Q}_B, \quad (\text{E.9})$$



with  $A \in \mathbf{a}$  and  $B \in \mathbf{b}$ . The sums are over all the momentum states and all the loops for the current partition. For the case  $r = 1/2$  the same form is obtained but with

$$\begin{aligned} \tilde{Q}_{AB,\gamma\alpha} \equiv & Q_{A,\gamma} \sqrt{\frac{(N_{\mathbf{a}'_\alpha} + n_A)!(N_{\mathbf{a}} - n_A)!}{N_{\mathbf{a}'_\alpha}!N_{\mathbf{a}}!}} \\ & - Q_{B,\gamma} \sqrt{\frac{(N_{\mathbf{b}'_\alpha} + n_B)!(N_{\mathbf{b}} - n_B)!}{N_{\mathbf{b}'_\alpha}!N_{\mathbf{b}}!}}. \end{aligned} \quad (\text{E.10})$$

Note that the minimum image convention was applied to  $\tilde{Q}_{AB}$ , although this is no more than a crude attempt to account for periodic boundary conditions.

It can be seen in Table III that this rigid subset algorithm with  $r = 1$  gets the ground state occupancy correct, as well as the occupancies of the first several excited states. (The dissipative transitions, Eq. (C.4), roughly correspond to  $r = 1$ ,  $g(n_A) = \delta_{n_A,1}$ , and  $\lambda = 1/10$ .) There are some relatively minor finite size effects evident. The viscosity for  $N = 1,000$ ,  $\eta^*(6) = 32.6(75)$ , is larger than that estimated in the text with the rigid-body algorithm  $\eta^*(6) = 16.3(75)$ , or corrected in Appendix D,  $\eta^*(6) = 22.9(42)$ , but it is nevertheless about a factor of 2 smaller than the classical result,  $\eta^*(6) = 71(24)$ . As mentioned the expression for the shear viscosity is not compatible with periodic boundary conditions in the condensed regime where the rate of change of momentum is not given by Newton's second law.

The case  $r = 1/2$  was quite unsatisfactory. It was found that the majority of the bosons in the system condensed into the momentum ground state, whereas for ideal bosons it is less than 10%. It is unclear why  $r = 1/2$  performed so poorly.

Evidently the quantitative simulation of the shear viscosity in the quantum condensed regime is a work in progress. Nevertheless, the qualitative understanding of the molecular origin of superfluidity is clear from the present analysis. The shear viscosity is much reduced or practically zero for condensed bosons because Newton's second law no longer holds: the rate of change of momentum due to an applied force is exponentially smaller in the condensed compared to the non-condensed regime. These quantum molecular dynamics equations are necessary for the equilibrium system to evolve at constant entropy, as demanded by fundamental statistical considerations (Attard 2012a Ch. 7), and as confirmed by the thermodynamic analysis of fountain pressure measurements of superfluid helium (Attard 2025 §4.6). In addition, the applied force effective on an individual boson is the shared non-local force, which is reduced from the individual classical force by averaging over the subset to which the boson belongs.

## Appendix F: Soft Wall Boundaries

As mentioned above, there are problems with calculating the viscosity for a system with periodic boundary

conditions. In the classical case, one can formulate the expression for the rate of change of the first momentum moment to depend on the product of the pair separation and the pair force. When the pair separation is calculated with the minimum image convention, then the viscosity is reasonable and insensitive to the system size.

For the quantum case in the condensed regime, the contribution from the change in occupation entropy precludes this product. The minimum image convention for  $\tilde{Q}_{AB}$  is unjustified other than as a crude approximation that works in the classical limit.

The reason for invoking the minimum image convention for periodic boundary conditions is that a boson near a boundary, say  $q_{jx} = L^-/2$ , in a positive momentum state moves to  $q_{jx} = -L^+/2$  in a single time step. This creates a discontinuous change in the momentum moment,  $\Delta P_{xy} = -\tau L p_{jy}/m$ . The minimum image separation is the smallest separation between one boson and another and its periodic replicas, and it has no such discontinuity in its evolution.

Periodic boundary conditions are useful because the subsystem assumes a uniform density profile and closely approximates a bulk homogeneous system. An alternative is boundary walls. In the thermodynamic limit the contribution from the walls is relatively negligible, and the system approximates a bulk homogeneous system. One can accelerate the progress to the limit by taking the walls to be a featureless semi-infinite half-space composed of the same material as the subsystem at the desired uniform density.

For the case of the Lennard-Jones pair potential,  $u(r) = 4\epsilon[(\sigma/r)^{12} - (\sigma/r)^6]$ , the corresponding one-body wall potential is

$$U_{\text{LJ}}^{\text{wall}}(h) = 2\pi\rho\sigma^3 4\epsilon \left[ \frac{\sigma^9}{90h^9} - \frac{\sigma^3}{12h^3} \right], \quad (\text{F.1})$$

where  $h$  is the distance to the wall and  $\rho$  is the nominal number density. In practice for a cubic subsystem of edge length  $L$ , the one-body potential for each boson is

$$U^{(1)}(\mathbf{q}_j) = \sum_{\alpha=x,y,z} U_{\text{LJ}}^{\text{wall}}(L/2 - q_{j\alpha}) + U_{\text{LJ}}^{\text{wall}}(q_{j\alpha} - L/2). \quad (\text{F.2})$$

In the simulations reported next, the pair potential was set to zero for separations beyond  $R^{\text{cut}} = 3.5\sigma$  (as was also the case for the results earlier in this paper), but no cut-off was applied to the wall potential. To partially compensate for the adsorption decrement at the walls, the edge length was chosen larger than in the case of periodic boundary conditions, namely  $L = (N/\rho)^{1/3} + 2w$ , with  $w \approx \sigma$ . With this value of  $w$ , the actual density in the center of the subsystem is slightly larger than the nominal density for the classical case, and slightly smaller in the quantum case.

The downside of using soft-wall boundary conditions is that the density profile is inhomogeneous in the vicinity of the walls (and edges and corners), and the approach to the thermodynamic limit can be expected to

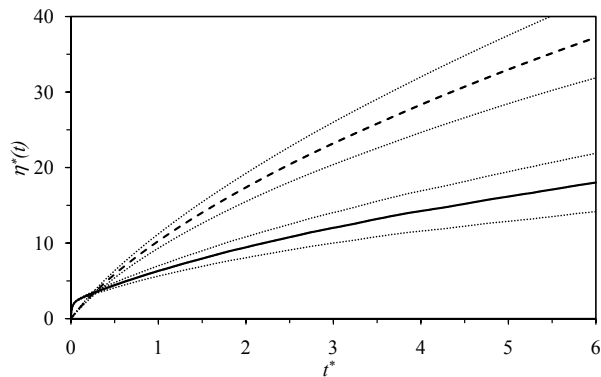


FIG. 9: Shear viscosity time function for Lennard-Jones liquid  ${}^4\text{He}$  with walls at  $T^* = 0.60$ ,  $\rho^* = 0.8872$ . The solid curve is the quantum liquid, the dashed curve is the classical liquid, and the dotted curves give the 95% confidence level. Also,  $N = 1,000$ ,  $L = (N/\rho)^{1/3} + 2w$ ,  $w = \sigma$ ,  $\Delta_p = 2\pi\hbar/L_{\text{eff}}$ , and  $L_{\text{eff}} = (N/\rho)^{1/3}$ . Rigid subset adiabatic transitions, Eqs (E.3) and (E.5) with  $r = 1$  were used, together with quadratic dissipative transitions, Eq. (C.4), once every 10 time steps,  $\tau^* = 2 \times 10^{-5}$ .

be slower than for the case of periodic boundary conditions. The upside is that the present simulations run about five times faster due to there being much fewer neighbors within the pair potential cut-off for a boson near the wall than in the alternative case.

Of course, the other advantage of boundary walls is that the expression for the adiabatic rate of change of the first momentum moment is well-defined and readily justified, and it enables an unambiguous comparison of the quantum and classical viscosities.

The results in Fig. 9 use  $w = \sigma$  and  $\Delta_p = 2\pi\hbar/L_{\text{eff}}$ , with  $L_{\text{eff}} = (N/\rho)^{1/3}$ . This is the same as the value used for periodic boundary conditions, being in the present case  $10.4\sigma$ , which is a little less than the width of the region of non-zero density,  $11.2\sigma$ , compared to  $L = L_{\text{eff}} + 2w = 12.4\sigma$ . These gave in the quantum case  $\rho(0) =$

$0.83(1)$ ,  $N_{000} = 92.9(51)$ ,  $f_0 = 0.7424(2)$ , and  $\eta^*(6) = 18.0(39)$ . In the classical case they gave  $\rho(0) = 0.91(3)$ ,  $N_{000} = 2.437(4)$ ,  $f_0 = 0.50715(6)$ , and  $\eta^*(6) = 37.2(54)$ .

Notable points from these and other simulations are

- The classical and quantum results were obtained in separate runs of the same program, the only differences being that in the classical case stochastic transitions were made independently for each boson according to its individual force without any contribution from a change in occupation entropy. These were also the only differences in the calculation of the viscosity.
- The shared non-local force for rigid subsets ‘blunts’ the repulsive force and allows pairs of bosons to approach to smaller separations than classically. Hence for the quantum system, both the pressure and the potential energy are higher than for the classical system.
- Runs with  $N = 500$ ,  $1,000$ , and  $2,000$  showed no statistically significant variation in the viscosity.
- About three quarters of the bosons are condensed in the quantum case.
- The quantum viscosity is about half the classical viscosity.
- The two-fluid model of superfluidity —the quantum viscosity equals the classical viscosity times the fraction of uncondensed bosons in the quantum system— is qualitatively rather than quantitatively confirmed by these results.

Obviously the quantitative value of the viscosity is sensitive to the model, the central density, and to the size of the momentum states. But in all the cases explored, for the same model and parameters, the quantum viscosity was significantly less than the classical viscosity.